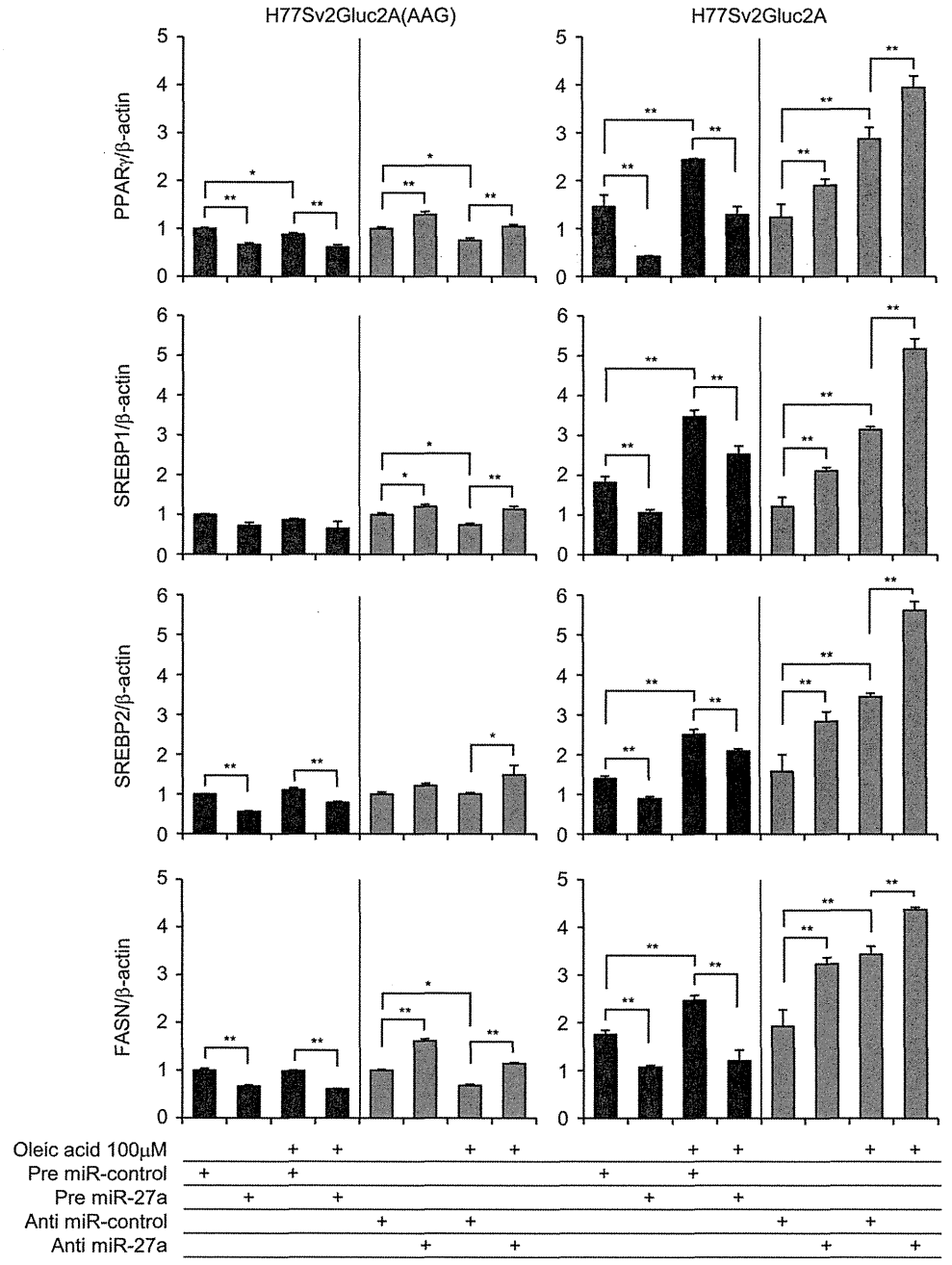

FIG 5 Expression of lipid metabolism-related transcription factors. Huh-7.5 cells were transfected with H77Sv2 Gluc2A RNA or H77Sv2 Gluc2A (AAG) RNA and pre- or anti-miR-27a. At 24 h posttransfection, oleic acid (100 μM) was added to the culture medium, and at 72 h after oleic acid treatment, *PPARγ*, *SREBP1*, *SREBP2*, and *FASN* expression levels were quantified by RTD-PCR ($n = 6$). Experiments were performed in duplicate and repeated three times. Values are means ± standard errors. *, $P < 0.01$; **, $P < 0.005$.

mRNA and protein levels (Fig. 5 and 6A and B). Pre-miR-27a significantly repressed the levels of these transcription factors and, conversely, anti-miR-27a significantly increased their mRNA and protein levels (Fig. 5 and 6A and B). This regulation by miR-27a was observed in both HCV-replicating and non-HCV-replicating cells, although the magnitude of the change was more prominent in HCV-replicating cells (Fig. 5).

As LDs associate with the ER-derived membrane at the site of HCV replication (10) and ER stress was recently shown to promote hepatic lipogenesis and LD formation (31), we next evaluated ER stress markers. Under HCV replication and lipid overload with oleic acid, anti-miR-27a increased the expression of the ER stress markers p-PERK, p-eIF2α, and BiP in Huh-7.5 cells. Conversely, pre-miR-27a significantly decreased the expression of these markers (Fig. 6C). Cell viability decreased after anti-miR-27a transfection and increased following pre-miR-27a treatment (Fig. 6D). Thus, miR-27a repressed the ER stress that was induced by HCV replication and lipid overload.

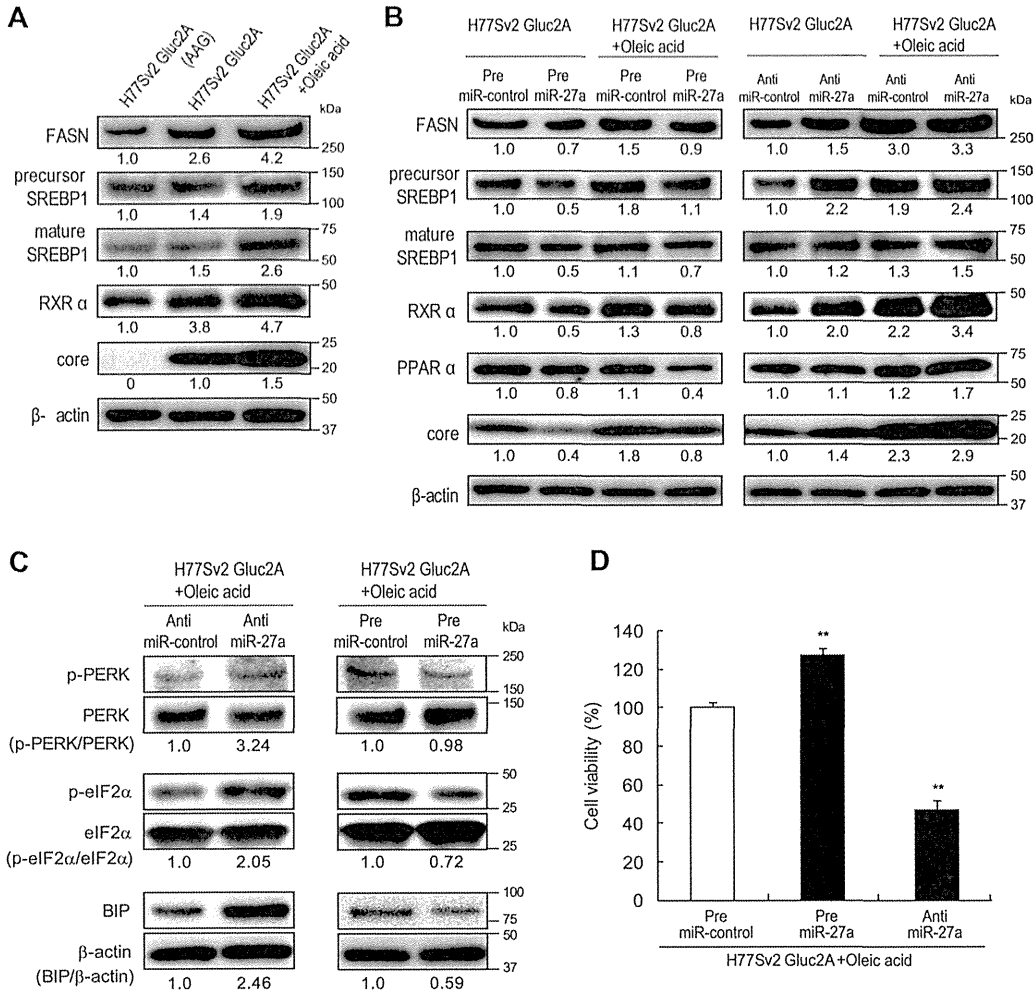

FIG 6 Expression of lipid metabolism-related transcription factors and ER stress-related factors. Huh-7.5 cells were transfected with H77Sv2 Gluc2A RNA or H77Sv2 Gluc2A (AAG) RNA and pre- or anti-miR-27a. At 24 h posttransfection, oleic acid (100 μM) was added to the culture medium. At 72 h after oleic acid treatment, the cells were harvested. (A) Western blotting of lipid metabolism-related transcription factors changed by HCV infection and oleic acid. Experiments were repeated three times. (B) Western blotting of lipid metabolism-related transcription factors changed by pre- or anti-miR-27a. Experiments were repeated three times. (C) Western blotting of ER stress-related transcription factors changed by pre- or anti-miR-27a. Experiments were repeated three times. (D) Cell viability in the same experiments was determined by MTS assay ($n = 9$). Experiments were performed in triplicate and repeated three times. Values are means ± standard errors. *, $P < 0.01$; **, $P < 0.005$.

miR-27a targets RXRα and the ATP-binding cassette transporter ABCA1. We next analyzed the expression of miR-27a target genes. A previous report showed that miR-27a targets RXRα in rat hepatic stellate cells (32), and we confirmed that miR-27a targets the 3′ UTR of human RXRα in Huh-7.5 cells (data not shown). Although the primary sequence of the human RXRα 3′ UTR shares approximately 60% homology with the corresponding rat sequence, the putative miR-27a binding site (ACUGUGAA) is conserved among several different species. Therefore, we constructed an expression vector containing a luciferase (Luc) reporter gene fused to the human RXRα 3′ UTR (pmirGLO-RXRα 3′ UTR) and reevaluated Luc activity (data not shown). Pre-miR-27a repressed Luc activity, while anti-miR-27a significantly increased Luc activity. The introduction of three nucleotide mutations into the conserved miR-27a binding site was shown to abolish these changes in Luc activity. These results confirmed previous findings that miR-27a targets RXRα (32). RXRα interacts with liver X receptor (LXR) and regulates many lipid synthetic genes such as *SREBP1* and *FASN*. We found that the expression of *SREBP1*, *FASN*, and *SREBP2* was regulated by miR-27a (Fig. 6B) and confirmed that *PPARγ* was also regulated by miR-27a, as reported previously (Fig. 5) (33). In addition, *PPARα* was shown to be regulated by miR-27a (Fig. 6B).

We next evaluated the expression of lipid transporter genes. The ATP-binding cassette transporter ABCA1 is mutated in Tangier's disease (34) and plays an important role in the efflux of TCHO for high-density lipoprotein (HDL) synthesis (35). A recent report demonstrated a functional role for ABCA1 in hepatocyte TG secretion to the plasma and in the reduction of cellular TG levels (29). Here we found that pre-miR-27a significantly repressed ABCA1 and, conversely, that anti-miR-27a increased the mRNA and protein levels of ABCA1 (Fig. 7A and B). We identified two miR-27a binding sites (sites 1 and 2) in the 3′ UTR of ABCA1 (Fig. 7C) that were conserved between species (Fig. 7C). An expression vector containing the *luc* reporter gene fused to the human ABCA1 3′ UTR (wild type [WT]) was constructed, and a

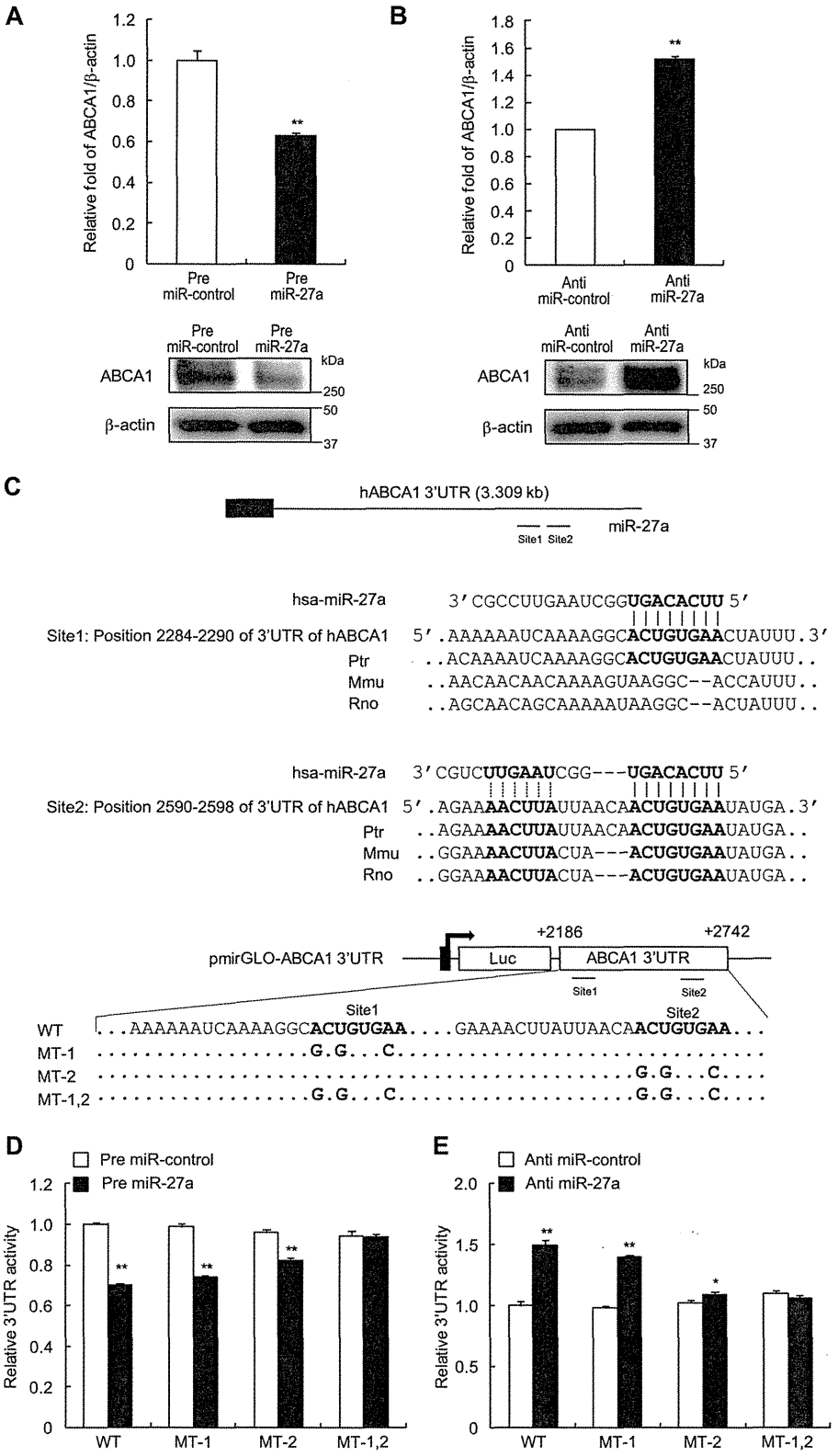

FIG 7 miR-27a targets ABCA1. (A) Regulation of ABCA1 by pre-miR-27a. RTD-PCR and Western blotting of ABCA1 in Huh-7.5 cells at 72 h posttransfection with pre-miR-control and pre-miR-27a ($n = 6$). **, $P < 0.005$. (B) Regulation of ABCA1 by anti-miR-27a. RTD-PCR and Western blotting of ABCA1 in Huh-7.5 cells at 72 h posttransfection with pre-miR-control and anti-miR-27a ($n = 6$). **, $P < 0.005$. (C) Sequence alignment of the ABCA1 3′ UTR and the construction of the luciferase (Luc) expression vector fused to the ABCA1 3′ UTR. Ptr, *Pan troglodytes*; Mmu, *Mus musculus*; Rno, *Rattus norvegicus*; WT, Luc reporter vector with the WT ABCA1 3′ UTR (2186 to 2742); MT-1, Luc reporter vector with the site 1 mutation of the WT; MT-2, Luc reporter vector with the site 2 mutation of the WT; MT-1,2, Luc reporter vector with mutations at sites 1 and 2 of the WT. (D, E) Suppression (D) or induction (E) of Luc activity with the various mutations of the ABCA1 3′ UTR by pre-miR-27a. Huh-7.5 cells were transfected with pre- or anti-miR-control or pre- or anti-miR-27a, and WT, MT-1, MT-2, and MT-1,2. Luc activities were measured at 24 h posttransfection ($n = 6$). All experiments were performed in duplicate and repeated three times. Values are means ± standard errors. *, $P < 0.01$; **, $P < 0.005$.

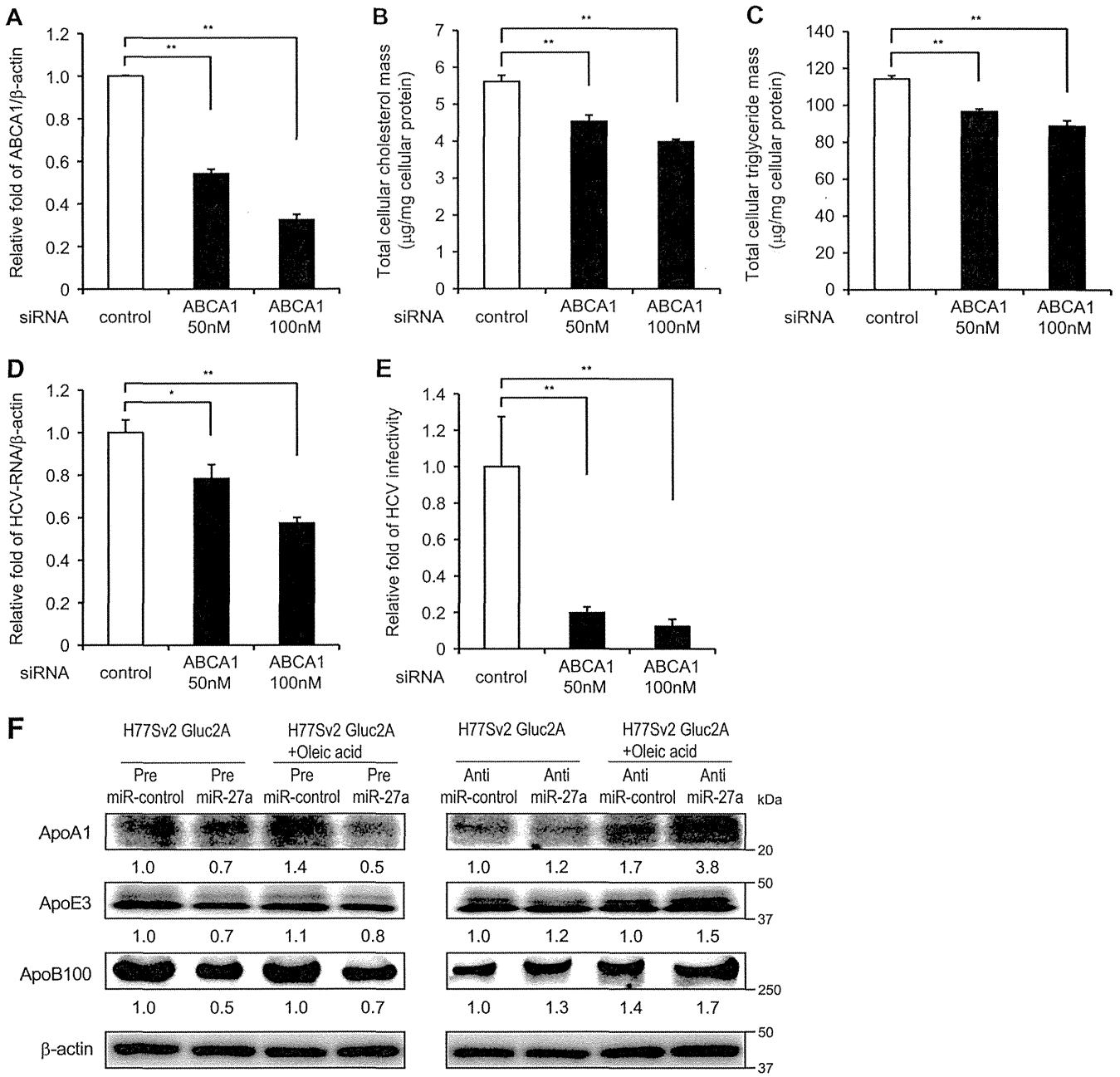

FIG 8 Suppression of ABCA1 inhibits HCV replication and infection. Huh-7.5 cells were transfected with H77Sv2 Gluc2A RNA and siRNA to ABCA1 or control siRNA. ABCA1 expression was quantified at 72 h posttransfection by RTD-PCR ($n = 6$). (A) Knockdown efficiency of ABCA1 in Huh-7.5 cells by siRNA. (B) TG concentration in cells ($n = 6$). (C) TCHO concentrations in cells ($n = 6$). (D) HCV RNA assay by RTD-PCR ($n = 6$). (E) HCV infectivity. Huh-7.5 cells were infected with HCVcc derived from ABCA1 knockdown Huh-7.5 cells. HCV RNA was quantified at 72 h postinfection by RTD-PCR ($n = 6$). Experiments were performed in duplicate and repeated three times. Values are means ± standard errors. *, $P < 0.01$; **, $P < 0.005$. (F) Regulation of ApoA1, ApoE2, and ApoB100 by miR-27a. Experiments were performed under the same conditions as Fig. 6B and C and repeated three times.

series of mutations were introduced into the putative miR-27a binding sites (MT-1, MT-2, and MT-1,2). The Luc activity of the WT was significantly repressed by pre-miR-27a and increased by anti-miR-27a. However, there was a smaller change in Luc activity caused by pre- and anti-miR-27a in the single mutants (MT-1 and MT-2) and no change in Luc activity in the double mutant (MT-1,2) (Fig. 7D and E). These results show that miR-27a targets ABCA1 to decrease the lipid content of cells.

The functional relevance of ABCA1 in lipid metabolism and HCV replication in Huh-7.5 cells was examined by inhibiting ABCA1 with an siRNA (Fig. 8). siRNA to ABCA1 repressed the expression of ABCA1 in a dose-dependent manner (Fig. 8A). Under this condition, the cellular TG and TCHO levels decreased significantly (Fig. 8B and C) and HCV RNA levels also decreased to 57% of the control. More strikingly, HCV infectivity decreased to 12% of the control (Fig. 8D and E).

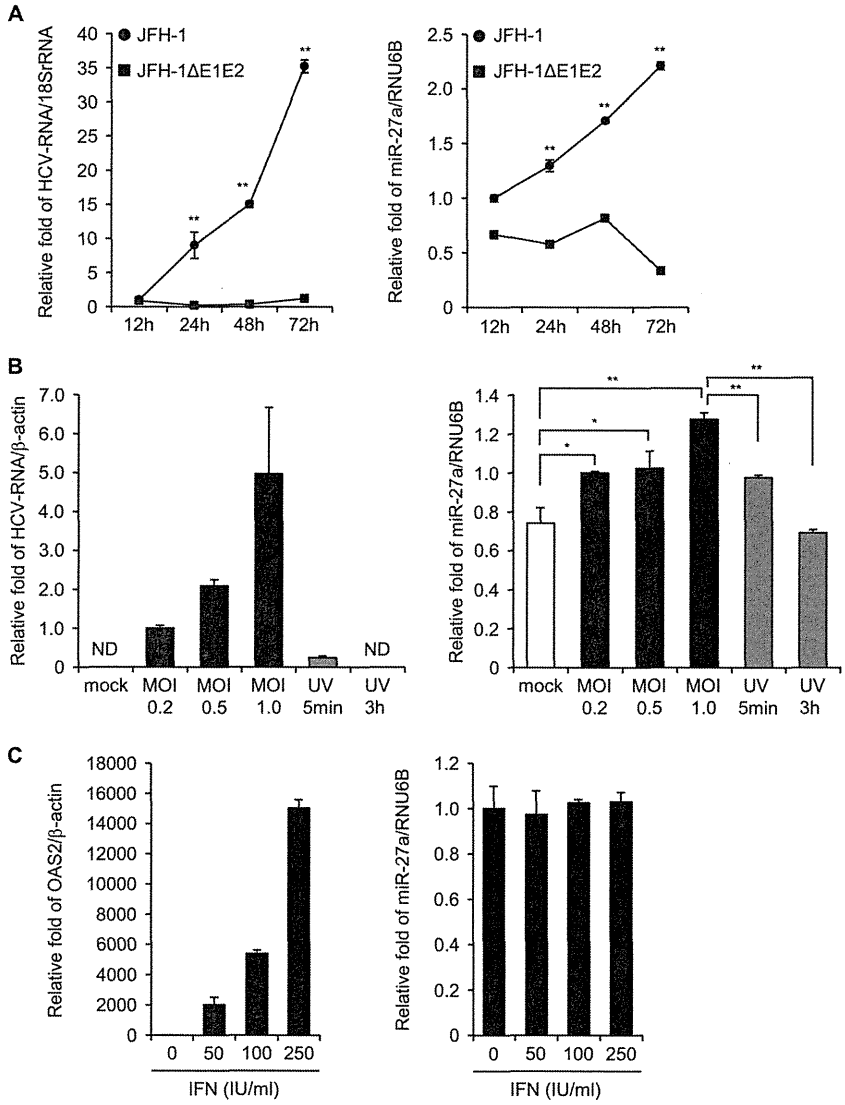

FIG 9 miR-27a is upregulated by HCV infection. (A) Kinetics of HCV replication and induction of miR-27a. Huh-7.5 cells were transfected with JFH-1 RNA or infection-incompetent JFH-1ΔE1E2 RNA (20). At 12, 24, 48, and 72 h posttransfection, HCV RNA (left) and miR-27a (right) levels were quantified by RTD-PCR ($n = 6$). (B) Induction of miR-27a and UV-irradiated HCV particles. Huh-7.5 cells were infected with infectious HCV (multiplicity of infection [MOI] of 0.2, 0.5, or 1) or UV-inactivated HCV. At 72 h postinfection, HCV RNA (left) and miR-27a (right) were quantified by RTD-PCR ($n = 6$). *, $P < 0.01$; **, $P < 0.005$; ND, not detected. (C) Induction of miR-27a and IFN-α treatment. Huh-7.5 cells were treated with different doses of IFN-α. At 24 h posttreatment, OAS2 (left) and miR-27a (right) were quantified by RTD-PCR ($n = 6$). All experiments were performed in duplicate and repeated three times. Values are means ± standard errors.

Several reports have demonstrated the importance of apolipoproteins, including the major components of VLDL and LDL apoE3 (36) and apoB100 (11), in the production of infectious HCV particles. More recently, the functional relevance of ApoA1 in HCV replication and particle production has been reported (37). Here the expression of apoA1, apoB100, and apoE3 was repressed by pre-miR-27a and increased by anti-miR-27a, suggesting that miR-27a regulates the expression of apolipoproteins to reduce the production of infectious HCV particles (Fig. 8F).

Regulation of miR-27a expression through C/EBPα. miR-27a forms a gene cluster with miR-23a and miR-24-2, and both of these miRNAs are regulated by the same promoter (38). However, no detailed analysis of the regulation of this promoter has been carried out. Because the expression of miR-27a was upregulated more in CH-C liver than CH-B liver, it could be speculated that HCV infection induces the expression of miR-27a. To examine this, we evaluated the expression of miR-27a during HCV infection (Fig. 9). The expression of miR-27a increased, correlating with the increase in JFH-1 RNA, while infection-incompetent JFH-1ΔE1E2 did not induce miR-27a expression (Fig. 9A). In addition, UV-irradiated HCV particles did not induce miR-27a expression (Fig. 9B). However, IFN-α treatment did not induce the expression of miR-27a (Fig. 9C). Thus, HCV infection was essential for induction of miR-27a expression.

We identified a C/EBPα binding site (−614 to −606), a key regulator of adipocyte differentiation, in the promoter region of miR-27a. Interestingly, H77Sv2 Gluc2A and tunicamycin

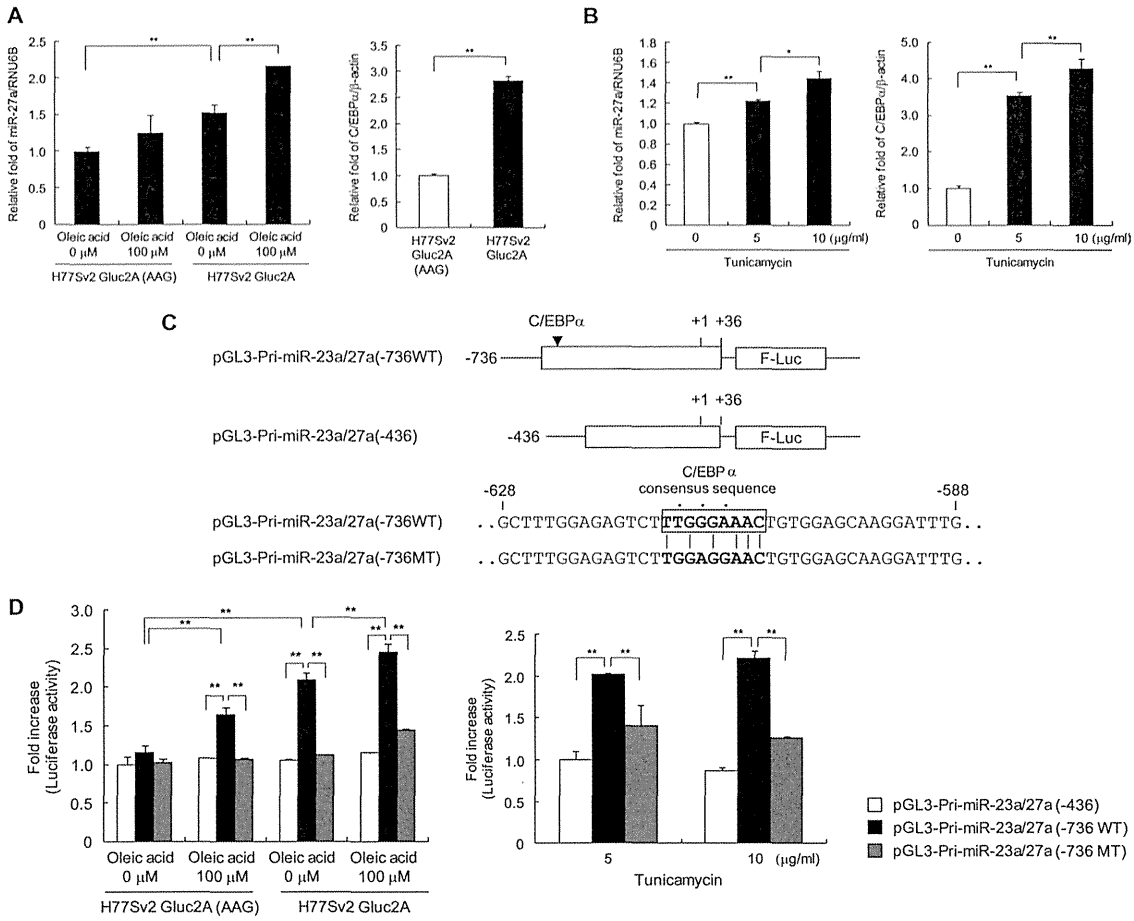

FIG 10 miR-27a is regulated by the adipocyte differentiation factor C/EBPα. (A) Induction of miR-27a and C/EBPα expression by oleic acid and HCV replication. Huh-7.5 cells were transfected with H77Sv2 Gluc2A RNA or H77Sv2 Gluc2A (AAG) RNA. At 24 h posttransfection, oleic acid (100 μM) was added to the culture medium. At 72 h after oleic acid treatment, miR-27a (left) and C/EBPα (right) levels were quantified by RTD-PCR ($n = 6$). (B) Induction of miR-27a and C/EBPα expression by tunicamycin. Huh-7.5 cells were treated with different doses of tunicamycin. At 24 h after tunicamycin treatment, miR-27a (left) and C/EBPα (right) levels were quantified by RTD-PCR ($n = 6$). (C) miR-27a promoter luciferase constructs. pGL3-Pri-miR-23a/27a(−736WT) includes −700 to +36 bp relative to the transcription initiation site of pri-miR-23a~27a~24-2. pGL3-Pri-miR-23a/27a (−436) includes −400 to +36 bp relative to the transcription initiation site of pri-miR-23a~27a~24-2, which lacks the consensus C/EBPα binding site. pGL3-Pri-miR-23a/27a(−736MT) has mutations at the −736WT C/EBPα binding site. (D) miR-27a promoter activity in Huh-7.5 cells following HCV infection and oleic acid (left) or tunicamycin (right) treatment. Reporter constructs lacking the C/EBPα binding site did not respond to any of these conditions ($n = 6$). All experiments were performed in duplicate and repeated three times. Values are means ± standard errors. *, $P < 0.01$; **, $P < 0.005$.

significantly induced the expression of miR-27a and C/EBPα (Fig. 10A and B). To analyze the induction of miR-27a through C/EBPα, we constructed a Luc reporter construct that included the upstream promoter region (−736) of miR-27a [pGL3-Pri-miR-23a/27a(−736WT)] together with a short promoter construct (−436) lacking the C/EBPα binding site [pGL3-Pri-miR-23a/27a(−436)]. In addition, three nucleotide mutations were introduced into the C/EBPα consensus binding site to construct pGL3-Pri-miR-23a/27a(−736MT) (Fig. 10C). The activity of pGL3-Pri-miR-23a/27a(−736WT), but not that of pGL3-Pri-miR-23a/27a(−736MT) or pGL3-Pri-miR-23a/27a(−436), which both lack a C/EBPα binding site, was induced by HCV replication, lipid overload, and tunicamycin treatment (Fig. 10D). These results indicate that the regulation of miR-27a by HCV replication, lipid overload, and ER stress is mediated through C/EBPα.

Pre-miR-27a enhances IFN signaling through the reduction of lipid storage. Finally, we assessed whether miR-27a influences IFN signaling. IFN-α treatment stimulated IFN signaling in a dose-dependent manner by increasing p-STAT1 expression in Huh-7.5 cells (Fig. 11A). Oleic acid impaired this induction of p-STAT1, while pre-miR-27a restored the expression of p-STAT1 and anti-miR-27a impaired this induction by oleic acid. These findings were observed in both HCV-replicating and non-HCV-replicating cells (Fig. 11A).

HCV replication deduced from Gluc activity is shown in Fig. 11B. IFN sensitivity could be estimated by the relative fold changes in Gluc activity from the baseline activity (in the absence of IFN). The results demonstrated that oleic acid reduced IFN sensitivity, while pre-miR-27a increased IFN sensitivity under either condition with or without oleic acid (Fig. 11B).

These findings were further studied with clinical samples. The expression of miR-27a was evaluated in liver biopsy specimens obtained from 41 patients who received pegylated IFN (Peg-IFN) and ribavirin (RBV) combination therapy (Fig. 12A). Interestingly, the expression of miR-27a was significantly higher

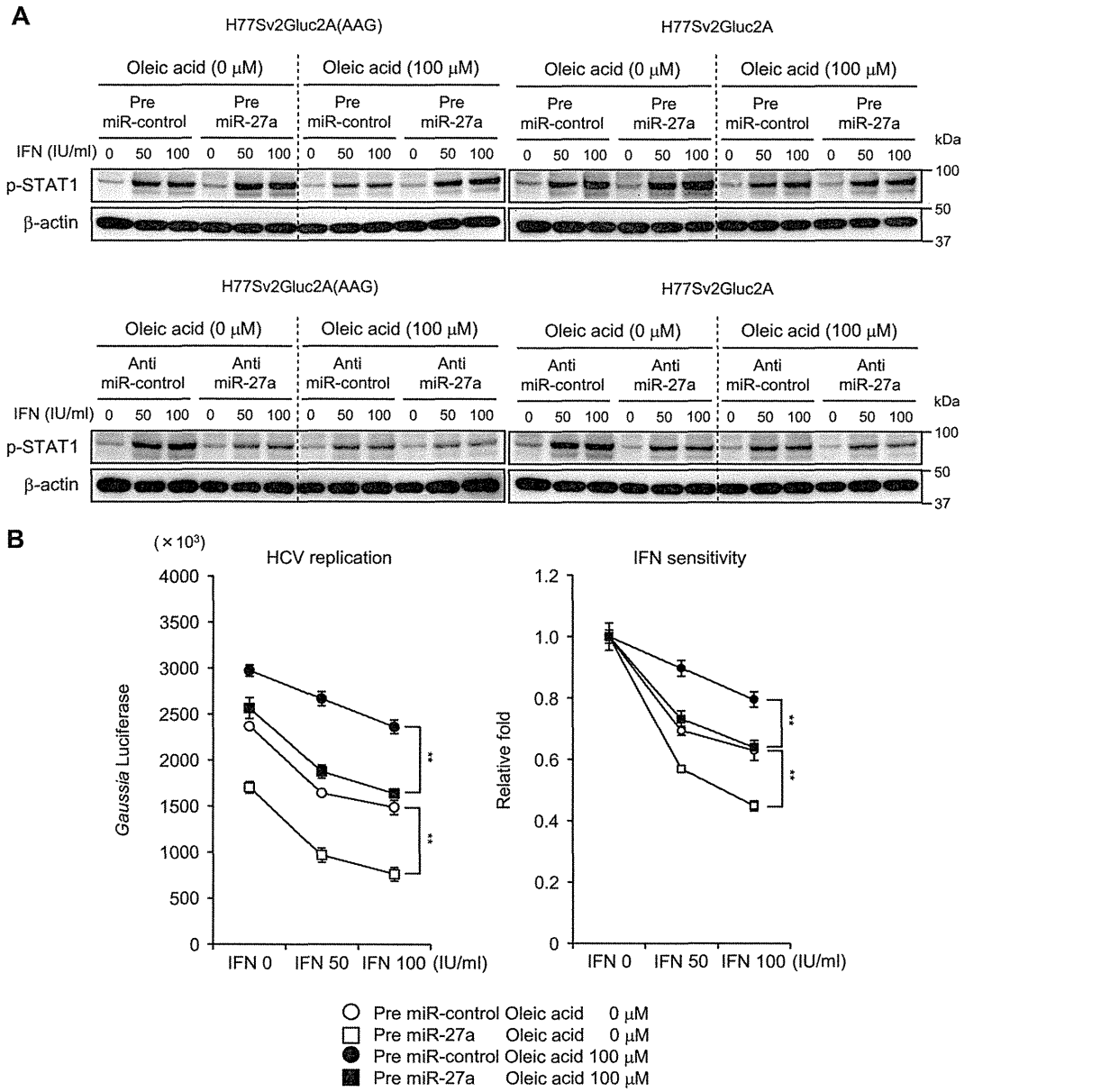

FIG 11 miR-27a restores IFN signaling impaired by lipid overload. (A) Induction of p-STAT1 expression by miR-27a. Huh-7.5 cells were transfected with H77Sv2 Gluc2A RNA or H77Sv2 Gluc2A (AAG) RNA and pre- or anti-miR-control or pre- or anti-miR-27a. At 24 h posttransfection, oleic acid (100 μM) was added to the culture medium. At 48 h after oleic acid treatment, the cells were treated with different doses of IFN-α. At 24 h after IFN treatment, p-STAT1 expression levels were determined by Western blotting. Experiments were repeated three times. (B) Absolute values of Gluc activity (left) and *n*-fold changes in Gluc activity (right) indicate IFN sensitivity ($n = 6$). Experiments were performed in duplicate and repeated three times. Values are means ± standard errors. *, $P < 0.01$; **, $P < 0.005$.

in patients with severe steatosis (grade 3 or 4) than in those with mild steatosis (grade 1 or 2) (Fig. 12B). Importantly, patients with a favorable response to treatment (sustained virological response or transient response) expressed higher miR-27a levels than patients with a poor response (nonresponse) (Fig. 12C). Although there was no significant difference in miR-27a expression according to the interleukin-28B (IL-28B) genotype (Fig. 12D and E), 17 patients had a treatment-resistant IL-28 genotype (TG at rs8099917) (39–41) and 6 of these with a favorable response to treatment expressed significantly higher miR-27a levels than the 11 with a poor response (Fig. 12E). These data suggest that miR-27a enhances IFN signaling and increases the response to IFN treatment.

DISCUSSION

Previously, we examined miRNA expression in HCC and noncancerous background liver tissue infected with HBV and HCV and showed the presence of infection-specific miRNAs that were differentially expressed according to HBV or HCV infection, but not according to the presence of HCC (2). In this study, we pursued the functional analysis of these miRNAs. Among 19 infection-specific miRNAs, we first focused on 6 that were upregulated by

A

No.	Age	Sex	Histological stage			Treatment response			IL28B SNP	
		M:F	F1	F2	F3	SVR	TR	NR	TT	TG
41	54.9±11.2	22:19	15	15	11	17	9	15	24	17

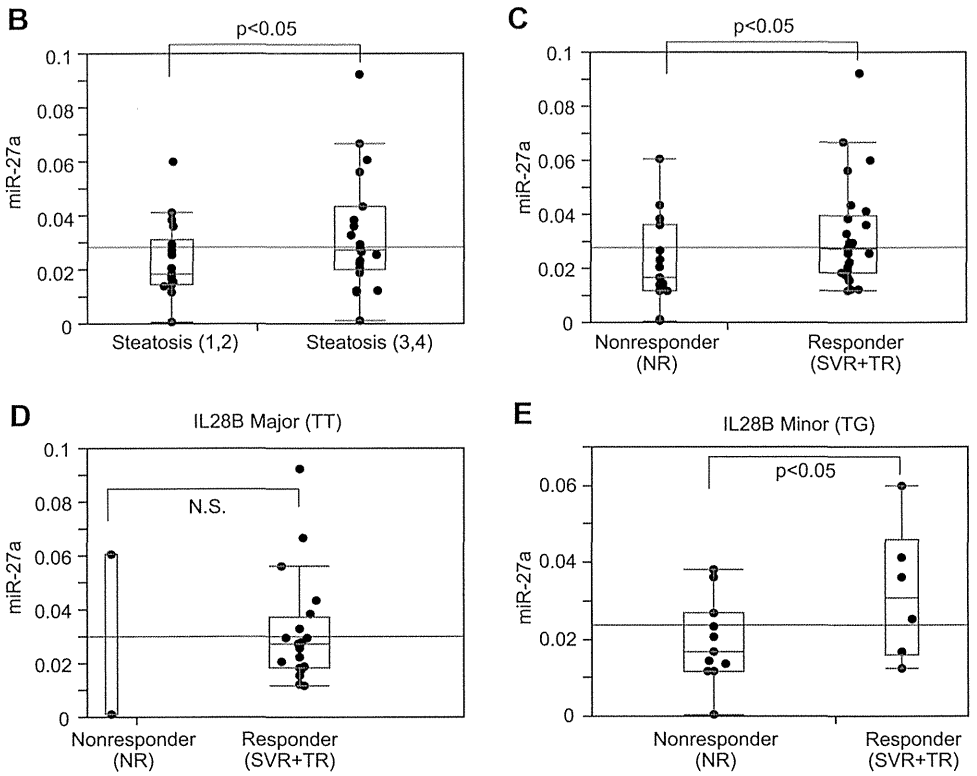

FIG 12 Expression of miR-27a in clinical samples. (A) Clinical characteristics of 41 patients who received Peg-IFN and RBV combination therapy. M:F, male/female ratio; SVR, sustained virological response; TR, transient response; NR, nonresponse; SNP, single nucleotide polymorphism. (B) Significant upregulation of miR-27a expression in the livers of patients with severe steatosis. Steatosis grades 1 and 2, $n = 19$; steatosis grades 3 and 4, $n = 22$. (C) Significant upregulation of miR-27a expression in the livers of patients with a favorable response to treatment (SVR or TR). Nonresponders; $n = 15$; responders, $n = 26$. (D) No significant difference in miR-27a expression between nonresponders and responders of the IL-28B major genotype (treatment-sensitive genotype) was observed. Nonresponders, $n = 3$; responders, $n = 21$. N.S., not significant. (E) Significant upregulation of liver miR-27a was observed in responders of the IL-28B minor genotype (treatment-resistant genotype). Nonresponders, $n = 11$; responders, $n = 6$.

HCV infection, as they were expected to have a positive role in HCV replication. However, inhibition experiments with a series of specific anti-miRNAs showed an unexpected increased in HCV replication. Closer examination clarified that miR-27a had a negative effect on HCV replication. Interestingly, profiling of gene expression in Huh-7.5 cells in which miR-27a was inhibited or overexpressed showed that miR-27a could target lipid metabolism signaling pathways. In support of these findings, the lipid content (TG and TCHO) of Huh-7.5 cells was significantly increased by anti-miR-27a and repressed by pre-miR-27a (Fig. 2 and 3). More importantly, miR-27a was involved in HCV particle formation, as demonstrated by iodixanol gradient centrifugation (Fig. 4). Anti-miR-27a reduced the buoyant density of HCV particles and increased HCV replication and infectivity, while pre-miR-27a decreased HCV replication and dramatically repressed HCV infectivity. In the buoyant-density experiment, the infectious HCV peaks were identical to the RNA peak and the lower infectious virus peak was not observed. We cannot explain this discrepancy from other studies; however, the method used to purify the virus particles could be one reason.

miR-27a regulated many lipid metabolism-related transcription factors, such as RXRα, PPARα, PPARγ, FASN, SREBP1, and SREBP2 (Fig. 5 and 6). We also confirmed that miR-27a targets RXRα in human Huh-7.5 cells, which is concordant with a previous study showing that miR-27a targets RXRα in rat hepatic stellate cells (32). Moreover, we newly demonstrated that the gene for the lipid transporter ABCA1 is a target of miR-27a. ABCA1 mediates the efflux of TCHO and phospholipids to the lipid-poor apolipoproteins ApoA1 and ApoE, which then form nascent HDLs (34, 35). It also mediates the transport of lipids between the Golgi apparatus and the cell membrane. Recently, the knockdown of ABCA1 in rat hepatoma cells increased TG secretion to the culture medium and decreased the cellular levels of FFA (29), while liver-specific ABCA1 knockout mice fed a high-fat diet showed increased plasma TG concentrations and decreased TG and TCHO contents in the liver (42). Thus, ABCA1 regulates the lipid content

of hepatocytes, as well as HDL synthesis. In this study, we confirmed that the repression of ABCA1 decreased cellular TG and TCHO levels in Huh-7.5 cells and, importantly, decreased HCV replication and strikingly repressed HCV infection (Fig. 8).

LXR/RXRα was previously shown to activate the ABCA1 promoter (34), but we clearly demonstrated here that miR-27a directly targets ABCA1. Pre-miR-27a repressed the Luc activity of a reporter construct fused with the ABCA1 3′ UTR, while anti-miR-27a increased it. We also found that miR-27a regulates the expression of ABCA1 in a 3′ UTR sequence-specific manner, as a series of mutations introduced into putative miR-27a binding sites abrogated its regulation (Fig. 7). In addition to these findings, we showed that miR-27a repressed the expression of the apolipoproteins ApoA1, ApoB100, and ApoE3, which were recently shown to play important roles in the production and formation of infectious HCV particles (Fig. 8) (11, 36, 37). Thus, miR-27a may regulate lipid metabolism by reducing lipid synthesis and increasing lipid secretion from cells.

As the expression of miR-27a was upregulated more in CH-C liver than in CH-B liver, it is speculated that miR-27a expression is induced by HCV infection. Indeed, we clearly demonstrated that miR-27a expression was induced by HCV infection, lipid overload, and tunicamycin-induced ER stress (Fig. 9). Furthermore, the adipocyte differentiation-related transcription factor C/EBPα was involved in this regulation. A central role for C/EBPα in the development of adipose tissue has been suggested, as it was found to be sufficient to trigger the differentiation of preadipocytes into mature adipocytes (43). Thus, HCV infection might trigger lipogenesis in hepatocytes by inducing C/EBPα, as shown in this study. Conversely, the induction of C/EBPα expression by miR-27a had a negative effect on lipogenesis and HCV replication. Therefore, miR-27a might play a negative feedback role in HCV infection-induced lipid storage in hepatocytes. Moreover, HCV replication might be hampered by HCV-induced miR-27a, which would partially explain the low HCV titer in CH-C liver.

Besides the anti-HCV effect of miR-27a observed in this study, an antivirus effect against murine cytomegalovirus (MCMV) infection was observed previously (44, 45). MCMV replication was initiated by miR-27a degradation from a viral transcript, while miR-27a had a negative effect on MCMV replication. It was also reported that miR-27a was the target of *Herpesvirus saimiri* U-rich RNAs and was downregulated in transformed T lymphocytes (46). Therefore, the functional relevance of miR-27a in transformed T cells should be explored in a future study. In this study, miR-27a was upregulated by HCV infection, which is in sharp contrast to MCMV and *H. saimiri* infection. Therefore, the differences in antiviral action and host cell interactions also need to be explored further.

Our assessment of miR-27a expression in patients receiving Peg-IFN and RBV combination therapy showed that those with high miR-27a levels had a more favorable treatment response (Fig. 12). Moreover, miR-27a significantly enhanced IFN signaling (Fig. 11), suggesting that it might have therapeutic benefits in combination with IFN therapy, especially in patients with the IFN-resistant IL-28B genotype, who show a more severe steatosis than those with the IFN-sensitive IL-28B genotype (39–41). Further studies should be performed to confirm these findings with more clinical samples.

Although miR-27a has been shown to be upregulated in cancers of the breast, kidney, ovary, and gastric region, its downregulation has been reported in colorectal cancer, malignant melanoma, oral squamous cell carcinoma, and acute promyelocytic leukemia (47). However, its importance in HCC remains controversial, with one report observing its upregulation compared with the level in normal liver tissue (48), while another showed lower miR-27a expression in HCC than in paired nontumor tissues (49). Moreover, our previous findings on HBV-related and HCV-related HCC showed no miR-27a upregulation compared with the level in the paired background liver (1.14-fold, $P = 0.49$).

In summary, we have revealed the important role of miR-27a in HCV replication for the first time. These findings will be applicable in the improvement of the therapeutic effects of anti-HCV therapy, especially in patients showing treatment resistance and severe hepatic steatosis.

ACKNOWLEDGMENTS

We thank Mina Nishiyama and Masayo Baba for their excellent technical assistance.

We have no potential competing interests to declare.

REFERENCES

1. **Esteller M.** 2011. Non-coding RNAs in human disease. Nat. Rev. Genet. 12:861–874.
2. **Ura S, Honda M, Yamashita T, Ueda T, Takatori H, Nishino R, Sunakozaka H, Sakai Y, Horimoto K, Kaneko S.** 2009. Differential microRNA expression between hepatitis B and hepatitis C leading disease progression to hepatocellular carcinoma. Hepatology 49:1098–1112.
3. **André P, Komurian-Pradel F, Deforges S, Perret M, Berland JL, Sodoyer M, Pol S, Brechot C, Paranhos-Baccala G, Lotteau V.** 2002. Characterization of low- and very-low-density hepatitis C virus RNA-containing particles. J. Virol. 76:6919–6928.
4. **Thomssen R, Bonk S, Propfe C, Heermann KH, Kochel HG, Uy A.** 1992. Association of hepatitis C virus in human sera with beta-lipoprotein. Med. Microbiol. Immunol. 181:293–300.
5. **Thomssen R, Bonk S, Thiele A.** 1993. Density heterogeneities of hepatitis C virus in human sera due to the binding of beta-lipoproteins and immunoglobulins. Med. Microbiol. Immunol. 182:329–334.
6. **Agnello V, Abel G, Elfahal M, Knight GB, Zhang QX.** 1999. Hepatitis C virus and other Flaviviridae viruses enter cells via low density lipoprotein receptor. Proc. Natl. Acad. Sci. U. S. A. 96:12766–12771.
7. **Germi R, Crance JM, Garin D, Guimet J, Lortat-Jacob H, Ruigrok RW, Zarski JP, Drouet E.** 2002. Cellular glycosaminoglycans and low density lipoprotein receptor are involved in hepatitis C virus adsorption. J. Med. Virol. 68:206–215.
8. **Triyatni M, Saunier B, Maruvada P, Davis AR, Ulianich L, Heller T, Patel A, Kohn LD, Liang TJ.** 2002. Interaction of hepatitis C virus-like particles and cells: a model system for studying viral binding and entry. J. Virol. 76:9335–9344.
9. **Shi ST, Lee KJ, Aizaki H, Hwang SB, Lai MM.** 2003. Hepatitis C virus RNA replication occurs on a detergent-resistant membrane that cofractionates with caveolin-2. J. Virol. 77:4160–4168.
10. **Miyanari Y, Atsuzawa K, Usuda N, Watashi K, Hishiki T, Zayas M, Bartenschlager R, Wakita T, Hijikata M, Shimotohno K.** 2007. The lipid droplet is an important organelle for hepatitis C virus production. Nat. Cell Biol. 9:1089–1097.
11. **Huang H, Sun F, Owen DM, Li W, Chen Y, Gale M, Jr, Ye J.** 2007. Hepatitis C virus production by human hepatocytes dependent on assembly and secretion of very low-density lipoproteins. Proc. Natl. Acad. Sci. U. S. A. 104:5848–5853.
12. **Bressler BL, Guindi M, Tomlinson G, Heathcote J.** 2003. High body mass index is an independent risk factor for nonresponse to antiviral treatment in chronic hepatitis C. Hepatology 38:639–644.
13. **Poynard T, Ratziu V, McHutchison J, Manns M, Goodman Z, Zeuzem S, Younossi Z, Albrecht J.** 2003. Effect of treatment with peginterferon or interferon alfa-2b and ribavirin on steatosis in patients infected with hepatitis C. Hepatology 38:75–85.

14. Jopling CL, Yi M, Lancaster AM, Lemon SM, Sarnow P. 2005. Modulation of hepatitis C virus RNA abundance by a liver-specific MicroRNA. Science 309:1577–1581.
15. Murakami Y, Aly HH, Tajima A, Inoue I, Shimotohno K. 2009. Regulation of the hepatitis C virus genome replication by miR-199a. J. Hepatol. 50:453–460.
16. Hou W, Tian Q, Zheng J, Bonkovsky HL. 2010. MicroRNA-196 represses Bach1 protein and hepatitis C virus gene expression in human hepatoma cells expressing hepatitis C viral proteins. Hepatology 51:1494–1504.
17. Bandyopadhyay S, Friedman RC, Marquez RT, Keck K, Kong B, Icardi MS, Brown KE, Burge CB, Schmidt WN, Wang Y, McCaffrey AP. 2011. Hepatitis C virus infection and hepatic stellate cell activation downregulate miR-29: miR-29 overexpression reduces hepatitis C viral abundance in culture. J. Infect. Dis. 203:1753–1762.
18. Cheng JC, Yeh YJ, Tseng CP, Hsu SD, Chang YL, Sakamoto N, Huang HD. 2012. Let-7b is a novel regulator of hepatitis C virus replication. Cell. Mol. Life Sci. 69:2621–2633.
19. Bhanja Chowdhury J, Shrivastava S, Steele R, Di Bisceglie AM, Ray R, Ray RB. 2012. Hepatitis C virus infection modulates expression of interferon stimulatory gene IFITM1 by upregulating miR-130A. J. Virol. 86:10221–10225.
20. Wakita T, Pietschmann T, Kato T, Date T, Miyamoto M, Zhao Z, Murthy K, Habermann A, Kräusslich HG, Mizokami M, Bartenschlager R, Liang TJ. 2005. Production of infectious hepatitis C virus in tissue culture from a cloned viral genome. Nat. Med. 11:791–796.
21. Shetty S, Kim S, Shimakami T, Lemon SM, Mihailescu MR. 2010. Hepatitis C virus genomic RNA dimerization is mediated via a kissing complex intermediate. RNA. 16:913–925.
22. Che ML, Yan YC, Zhang Y, Gu Y, Wang NS, Chen N, Mao PJ, Zhang JY, Ding XQ, Yuan WJ, Mei CL, Yao J, Fan YL, Zhou Y, Zhang W, Zhu HW, Liu M, Jin HM, Qian JQ. 2009. Analysis of drug-induced acute renal failure in Shanghai. Zhonghua Yi Xue Za Zhi 89:744–749. (In Chinese.)
23. Shimakami T, Welsch C, Yamane D, McGivern DR, Yi M, Zeuzem S, Lemon SM. 2011. Protease inhibitor-resistant hepatitis C virus mutants with reduced fitness from impaired production of infectious virus. Gastroenterology 140:667–675.
24. Yi M, Villanueva RA, Thomas DL, Wakita T, Lemon SM. 2006. Production of infectious genotype 1a hepatitis C virus (Hutchinson strain) in cultured human hepatoma cells. Proc. Natl. Acad. Sci. U. S. A. 103:2310–2315.
25. Honda M, Takehana K, Sakai A, Tagata Y, Shirasaki T, Nishitani S, Muramatsu T, Yamashita T, Nakamoto Y, Mizukoshi E, Sakai Y, Nakamura M, Shimakami T, Yi M, Lemon SM, Suzuki T, Wakita T, Kaneko S. 2011. Malnutrition impairs interferon signaling through mTOR and FoxO pathways in patients with chronic hepatitis C. Gastroenterology 141:128–140.
26. Malhi H, Barreyro FJ, Isomoto H, Bronk SF, Gores GJ. 2007. Free fatty acids sensitise hepatocytes to TRAIL mediated cytotoxicity. Gut 56:1124–1131.
27. Honda M, Nakamura M, Tateno M, Sakai A, Shimakami T, Shirasaki T, Yamashita T, Arai K, Sakai Y, Kaneko S. 2010. Differential interferon signaling in liver lobule and portal area cells under treatment for chronic hepatitis C. J. Hepatol. 53:817–826.
28. Shirasaki T, Honda M, Mizuno H, Shimakami T, Okada H, Sakai Y, Murakami S, Wakita T, Kaneko S. 2010. La protein required for internal ribosome entry site-directed translation is a potential therapeutic target for hepatitis C virus replication. J. Infect. Dis. 202:75–85.
29. Chung S, Gebre AK, Seo J, Shelness GS, Parks JS. 2010. A novel role for ABCA1-generated large pre-beta migrating nascent HDL in the regulation of hepatic VLDL triglyceride secretion. J. Lipid Res. 51:729–742.
30. Lewis BP, Burge CB, Bartel DP. 2005. Conserved seed pairing, often flanked by adenosines, indicates that thousands of human genes are microRNA targets. Cell 120:15–20.
31. Lee JS, Mendez R, Heng HH, Yang ZQ, Zhang K. 2012. Pharmacological ER stress promotes hepatic lipogenesis and lipid droplet formation. Am. J. Transl. Res. 4:102–113.
32. Ji J, Zhang J, Huang G, Qian J, Wang X, Mei S. 2009. Over-expressed microRNA-27a and 27b influence fat accumulation and cell proliferation during rat hepatic stellate cell activation. FEBS Lett. 583:759–766.
33. Kim SY, Kim AY, Lee HW, Son YH, Lee GY, Lee JW, Lee YS, Kim JB. 2010. miR-27a is a negative regulator of adipocyte differentiation via suppressing PPARgamma expression. Biochem. Biophys. Res. Commun. 392:323–328.
34. Schmitz G, Langmann T. 2005. Transcriptional regulatory networks in lipid metabolism control ABCA1 expression. Biochim. Biophys. Acta 1735:1–19.
35. Liu M, Chung S, Shelness GS, Parks JS. 2012. Hepatic ABCA1 and VLDL triglyceride production. Biochim. Biophys. Acta 1821:770–777.
36. Hishiki T, Shimizu Y, Tobita R, Sugiyama K, Ogawa K, Funami K, Ohsaki Y, Fujimoto T, Takaku H, Wakita T, Baumert TF, Miyanari Y, Shimotohno K. 2010. Infectivity of hepatitis C virus is influenced by association with apolipoprotein E isoforms. J. Virol. 84:12048–12057.
37. Mancone C, Steindler C, Santangelo L, Simonte G, Vlassi C, Longo MA, D'Offizi G, Di Giacomo C, Pucillo LP, Amicone L, Tripodi M, Alonzi T. 2011. Hepatitis C virus production requires apolipoprotein A-I and affects its association with nascent low-density lipoproteins. Gut 60:378–386.
38. Lee Y, Kim M, Han J, Yeom KH, Lee S, Baek SH, Kim VN. 2004. MicroRNA genes are transcribed by RNA polymerase II. EMBO J. 23:4051–4060.
39. O'Brien TR. 2009. Interferon-alfa, interferon-lambda and hepatitis C. Nat. Genet. 41:1048–1050.
40. Suppiah V, Moldovan M, Ahlenstiel G, Berg T, Weltman M, Abate ML, Bassendine M, Spengler U, Dore GJ, Powell E, Riordan S, Sheridan D, Smedile A, Fragomeli V, Muller T, Bahlo M, Stewart GJ, Booth DR, George J. 2009. IL28B is associated with response to chronic hepatitis C interferon-alpha and ribavirin therapy. Nat. Genet. 41:1100–1104.
41. Tanaka Y, Nishida N, Sugiyama M, Kurosaki M, Matsuura K, Sakamoto N, Nakagawa M, Korenaga M, Hino K, Hige S, Ito Y, Mita E, Tanaka E, Mochida S, Murawaki Y, Honda M, Sakai A, Hiasa Y, Nishiguchi S, Koike A, Sakaida I, Imamura M, Ito K, Yano K, Masaki N, Sugauchi F, Izumi N, Tokunaga K, Mizokami M. 2009. Genome-wide association of IL28B with response to pegylated interferon-alpha and ribavirin therapy for chronic hepatitis C. Nat. Genet. 41:1105–1109.
42. Chung S, Timmins JM, Duong M, Degirolamo C, Rong S, Sawyer JK, Singaraja RR, Hayden MR, Maeda N, Rudel LL, Shelness GS, Parks JS. 2010. Targeted deletion of hepatocyte ABCA1 leads to very low density lipoprotein triglyceride overproduction and low density lipoprotein hypercatabolism. J. Biol. Chem. 285:12197–12209.
43. Porse BT, Pedersen TA, Xu X, Lindberg B, Wewer UM, Friis-Hansen L, Nerlov C. 2001. E2F repression by C/EBPalpha is required for adipogenesis and granulopoiesis in vivo. Cell 107:247–258.
44. Libri V, Helwak A, Miesen P, Santhakumar D, Borger JG, Kudla G, Grey F, Tollervey D, Buck AH. 2012. Murine cytomegalovirus encodes a miR-27 inhibitor disguised as a target. Proc. Natl. Acad. Sci. U. S. A. 109:279–284.
45. Marcinowski L, Tanguy M, Krmpotic A, Radle B, Lisnic VJ, Tuddenham L, Chane-Woon-Ming B, Ruzsics Z, Erhard F, Benkartek C, Babic M, Zimmer R, Trgovcich J, Koszinowski UH, Jonjic S, Pfeffer S, Dolken L. 2012. Degradation of cellular mir-27 by a novel, highly abundant viral transcript is important for efficient virus replication in vivo. PLoS Pathog. 8:e1002510. doi:10.1371/journal.ppat.1002510.
46. Cazalla D, Yario T, Steitz JA. 2010. Down-regulation of a host microRNA by a Herpesvirus saimiri noncoding RNA. Science 328:1563–1566.
47. Chhabra R, Dubey R, Saini N. 2010. Cooperative and individualistic functions of the microRNAs in the miR-23a~27a~24-2 cluster and its implication in human diseases. Mol. Cancer 9:232.
48. Huang S, He X, Ding J, Liang L, Zhao Y, Zhang Z, Yao X, Pan Z, Zhang P, Li J, Wan D, Gu J. 2008. Upregulation of miR-23a approximately 27a approximately 24 decreases transforming growth factor-beta-induced tumor-suppressive activities in human hepatocellular carcinoma cells. Int. J. Cancer 123:972–978.
49. Wang W, Zhao LJ, Tan YX, Ren H, Qi ZT. 2012. MiR-138 induces cell cycle arrest by targeting cyclin D3 in hepatocellular carcinoma. Carcinogenesis 33:1113–1120.

GASTROENTEROLOGY 2012;142:654-663

Peptidomimetic Escape Mechanisms Arise via Genetic Diversity in the Ligand-Binding Site of the Hepatitis C Virus NS3/4A Serine Protease

CHRISTOPH WELSCH,*,‡,§ TETSURO SHIMAKAMI,* CHRISTOPH HARTMANN,§ YAN YANG,*
FRANCISCO S. DOMINGUES,‖ THOMAS LENGAUER,§ STEFAN ZEUZEM,‡ and STANLEY M. LEMON*

*Division of Infectious Diseases, Department of Medicine, Inflammatory Diseases Institute, and the Lineberger Comprehensive Cancer Center, The University of North Carolina at Chapel Hill, Chapel Hill, North Carolina; ‡Department of Internal Medicine I, J. W. Goethe-University Hospital, Frankfurt, Germany; §Computational Biology and Applied Algorithmics, Max Planck Institute for Informatics, Saarbrücken, Germany; ‖Institute of Genetic Medicine, EURAC Research, Bolzano, Italy

BACKGROUND & AIMS: It is a challenge to develop direct-acting antiviral agents that target the nonstructural protein 3/4A protease of hepatitis C virus because resistant variants develop. Ketoamide compounds, designed to mimic the natural protease substrate, have been developed as inhibitors. However, clinical trials have revealed rapid selection of resistant mutants, most of which are considered to be pre-existing variants. **METHODS:** We identified residues near the ketoamide-binding site in x-ray structures of the genotype 1a protease, co-crystallized with boceprevir or a telaprevir-like ligand, and then identified variants at these positions in 219 genotype-1 sequences from a public database. We used side-chain modeling to assess the potential effects of these variants on the interaction between ketoamide and the protease, and compared these results with the phenotypic effects on ketoamide resistance, RNA replication capacity, and infectious virus yields in a cell culture model of infection. **RESULTS:** Thirteen natural binding-site variants with potential for ketoamide resistance were identified at 10 residues in the protease, near the ketoamide binding site. Rotamer analysis of amino acid side-chain conformations indicated that 2 variants (R155K and D168G) could affect binding of telaprevir more than boceprevir. Measurements of antiviral susceptibility in cell-culture studies were consistent with this observation. Four variants (ie, Q41H, I132V, R155K, and D168G) caused low-to-moderate levels of ketoamide resistance; 3 of these were highly fit (Q41H, I132V, and R155K). **CONCLUSIONS: Using a comprehensive sequence and structure-based analysis, we showed how natural variation in the hepatitis C virus protease nonstructural protein 3/4A sequences might affect susceptibility to first-generation direct-acting antiviral agents. These findings increase our understanding of the molecular basis of ketoamide resistance among naturally existing viral variants.**

Keywords: Virology; Genetic; Drug Resistance; Treatment.

Until recently, the standard of care (SOC) for patients with chronic hepatitis C virus (HCV) infection has consisted of a combination of pegylated interferon-alfa plus ribavirin (Peg-IFN/RBV) administered for 24 to 48 weeks, depending on HCV genotype.[1-3] The sustained virologic response rate for this SOC has been only about 50% in patients infected with genotype 1 HCV, the most prevalent genotype in Europe and North America. The addition of a direct-acting antiviral agent (DAA) targeting the nonstructural protein (NS) 3/4A serine protease of HCV significantly improves the sustained virologic response rate, and 2 such drugs have recently been approved for clinical use in Europe and the United States. The ketoamide compounds boceprevir (SCH503034) and telaprevir (VX-950) were both designed to mimic the natural substrate of the protease.[4-6] Clinical trials in treatment-naïve genotype 1-infected patients have revealed significant improvements in the kinetic of the virologic response with the addition of a DAA to the earlier SOC, leading to improved sustained virologic response rates of up to 74%.[7-9]

Unlike Peg-IFN/RBV, the selection of drug-resistant virus variants during treatment with protease inhibitors (PIs) is a major concern. According to recent calculations by Rong et al,[10] most, if not all, potential drug-resistant viral variants pre-exist at low frequencies within the viral quasi-species population in untreated patients. The highly replicative nature of HCV infection, with approximately 10^{12} new virions produced each day in the typical infected individual,[11] coupled with the lack of proofreading activity in the RNA-dependent RNA polymerase, NS5B, results in generation of every possible viral variant every day. Thus, each patient is infected with a viral quasi-species "cloud" comprised of genetically distinct but closely related viral genomes. In the absence of concomitant Peg-IFN/RBV therapy, drug-resistant viral variants are rapidly selected and can emerge at frequencies as high as 5% to 20% in the quasi-species of patients as early as the second day of treatment. Unless suppressed by concomitant PegIFN/RBV, these pre-existing resistant variants are likely to be selected with subsequent treatment failure.[10]

The NS3/4A protease plays an essential role in the HCV replication cycle by proteolytically processing nonstruc-

Abbreviations used in this paper: BSV, binding-site variant; DAA, direct-acting antiviral agent; EC_{50}, 50% effective concentration; GLuc, Gaussia luciferase; NS, nonstructural protein; PDB, Protein Databank; Peg-IFN/RBV, pegylated interferon-alfa plus ribavirin; PI, protease inhibitor; SOC, standard of care; TLL, telaprevir-like ligand.

0016-5085/$36.00
doi:10.1053/j.gastro.2011.11.035

tural proteins from the viral polyprotein downstream of the NS2-3 junction.[12] The protease domain of NS3, comprising the amino-terminal third of the protein contains a catalytic triad, H57, D81, and S139, and an "oxyanion hole" at G137. It acts in concert with its cofactor, NS4A, which intercalates into its structure and is required for full enzymatic activity and proper subcellular localization. The carboxy-terminal two thirds of NS3 comprises a DExD-box RNA helicase domain that is essential for productive viral infection.[13] NS3 appears to be a critical component of the macromolecular viral RNA replicase that directs the synthesis of new viral RNAs. Genetic evidence indicates that NS3 has an additional distinct function in the assembly of virus particles.[14,15] Because viral RNA replication capacity and virus assembly are crucial determinants of viral fitness, mutations in NS3 that contribute to PI resistance can also profoundly influence virus fitness.[16] The probability of a resistant variant emerging from the quasi-species population during treatment with a DAA is determined not only by its degree of resistance, but also by its fitness. Many mutations associated with PI resistance negatively impact the replication of genotype 1a HCV RNA in cell culture, while some have additional effects on the production of infectious virus.[14] Compensatory second-site mutations can enhance the fitness of resistant viruses,[16] but current understanding of these is rudimentary.

Given the genetic diversity that exists among different HCV strains, it is possible that naturally occurring polymorphisms in the NS3/4A sequence could provide a priori resistance to DAAs and negatively impact the success of future treatment regimens. Here, we have studied the variation in amino acid residues that neighbor ketoamide compounds in the ligand-binding site of the protease. We identified natural amino acid substitutions at these positions in NS3 among genotype 1a sequences deposited in a public database, and modeled their side-chain conformations to assess their potential impact on ketoamide binding. To corroborate these in silico predictions, we then introduced these amino acid substitutions into a cell culture-infectious genotype 1a virus (H77S.3)[14] and determined their impact on both susceptibility to ketoamide PIs and replication fitness in a cell culture system.

Materials and Methods

Details of the Materials and Methods can be found in the Supplementary Materials.

In Silico Analysis

We used x-ray structures of the genotype 1a HCV NS3/4A protease from the RCSB Protein Databank (PDB)[17] co-crystallized with boceprevir (PDB 2OC8) or a telaprevir-like ligand (TLL; PDB 2P59) to deduce sets of ketoamide-neighboring residues. We designated the P_4 to P_1 and P_1' groups for ligands and their corresponding specificity pockets within the ligand-binding site, S_4 to S_1 and S_1', according to the numbering scheme of Schechter and Berger.[18] We then analyzed 219 genotype 1a HCV NS3/4A sequences deposited in the European HCV database,[19] which contains sequences collected from around the world, to identify potential natural binding site variants (BSVs) at residues that neighbor the ketoamides within the structure of the protease. The side-chain conformations of these BSVs were modeled using IRECS (Iterative REduction of Conformational Space)[20] (details in Supplementary Material).

Cell Culture and Reagents

Details of the cells and reagents used in this study are provided in Supplementary Material.

Plasmids

The pH77S.3 and pH77S.3/Gaussia luciferase (GLuc)2A are molecular clones of the genotype 1a H77 strain of HCV. Synthetic RNA transcribed from these plasmids replicates in transfected Huh7 cells and produces infectious virus.[14] pH77S.3/GLuc2A RNA also produces secreted GLuc reporter protein. Amino acid substitutions in BSVs expected to impact ketoamide binding were created in these plasmids by site-directed mutagenesis.[14]

Virus Fitness and Antiviral Resistance

Genome-length RNA was transcribed from the mutated pH77S.3 and pH77S.3/GLuc2A plasmids in vitro, and studies to assess antiviral resistance and viral fitness carried out as described previously.[14]

Results

To identify amino acid residues in NS3 that are in close proximity to ketomides in the ligand-binding site of the protease, we analyzed PDB structure 2OC8 in which boceprevir is co-crystallized with the NS3/4A protease.[21] Because no similar co-crystallized structure is publically available for telaprevir, we used PDB structure 2P59 in which the protease is co-crystallized with a TLL that has 2 small differences from telaprevir.[22] Its P_2 group and the P_4 capping group are slightly modified, with the P_4 providing a pyrrole NH for H-bond interactions with the protease (Supplementary Figure 1).[23] We identified 20 residues interacting with or neighboring boceprevir and TLL in these x-ray structures (Table 1 and Supplementary Materials and Methods) and analyzed genotype 1a HCV sequences in the European HCV database to identify differences from the consensus sequence at these residues. The residues were relatively well conserved in 219 genotype 1a sequences from diverse geographic regions. However, we identified 13 different BSVs involving 10 ketoamide-neighboring residues (Supplementary Table 1 and Supplementary Figure 2), 8 of which have not been described previously as PI resistance-associated variants. None of the patients from whom these sequences were derived appear to have been treated previously with a DAA (see Supplementary Table 3). Most of these naturally occurring BSVs were single amino acid substitutions without changes in other ketoamide-neighboring residues. However, T42A and K136R were both present within a single sequence (EU677251). Two different BSVs were identified as substitutions at T42 (A/S), V55 (A/I), and D168 (G/E), while single BSVs were identified at the other 7 residues

Table 1. Ketoamide-Neighboring Residues in NS3[a]

Boceprevir		Telaprevir-like ligand	
RCSB PDB 2OC8 (chain B)	UniProtKB P27958	RCSB PDB 2P59 (chain B)	UniProtKB P27958
Q41	Q41	Q1067	Q41
T42	*T42*[b]	T1068	T42
F43	F43	F1069	F43
V55	*V55*	–	–
H57	H57	H1083	H57
D81	*D81*	*D1107*	*D81*
R123	R123	*R1149*	*R123*
I132	I132	I1158	I132
L135	L135	*L1161*	*L135*
K136	K136	K1162	K136
G137	G137	G1163	G137
S138	S138	S1164	S138
S139	S139	S1165	S139
F154	F154	F1180	F154
R155	R155	R1181	R155
A156	A156	A1182	A156
A157	A157	A1183	A157
V158	V158	V1184	V158
C159	C159	C1185	C159
	–	*T1186*	*T160*
D168	D168	D1194	D168

[a]Residues are numbered relative to the PDB residue sequence and H77c reference sequences (UniProtKB P27958).
[b]Residues shown in italics do not directly interact with boceprevir or TLL, but are within 5.0 Å distance of the ligand (see Supplementary Material).

(Supplementary Table 1 and Supplementary Figure 2). We examined the first-neighbor residues of these BSVs in an effort to identify potential second-site variants in the BSV strains (see Supplementary Material, Supplementary Figure 3, and Supplementary Table 2). Although there were no additional substitutions at these first-neighbor residues in most BSVs, T54S was found in both V55I strains (EF407443 and EU781818) and I170V was found in a R155K strain (EU781805).

Rotamer Analysis of BSVs and Expected Impact on Ketoamide Binding

We modeled the energetically most favorable side-chain conformations for the genotype 1a consensus and BSV sequences (Figure 1). Because V55 is buried in the protease domain,[24] it was not amenable to rotamer analysis. Molecular dynamics simulation of variants at this position will be reported separately (Welsch et al, Antimicrob Agents Chemother, accepted manuscript).

Expected impact of Q41H and K136R at the ketoamide P_1' position. Q41 is located adjacent to S_1'. The H41 variant represents a nonconservative change from the consensus sequence involving substitution of an uncharged polar side chain with a charged aromatic residue. Telaprevir possesses a cyclopropyl group at P_1' that is oriented away from the Q41 side chain without noncovalent interactions. The conformation of Q41 suggests a potential H-bond interaction of its carboxamide chain, including the H-bond donor NH_2 and acceptor C=O, with the backbone of boceprevir and TLL (OE1–HN distance for Q41-ketoamide: 2.7 Å). However, the H41 BSV has no side-chain group allowing an H-bond interaction with the ligand (Figure 2*A*). This suggests H41 will be associated with a minor decrease in binding affinity for boceprevir and telaprevir.

In contrast, K136R is a conservative change between polar residues, both with long, flexible, and charged side chains at S_1'. The K136 side chain is not defined in the electron density map of PDB structure 2P59. As modeled, it has close contacts with the TLL P_1' cyclopropyl group (Figure 2*B*). Boceprevir possesses no comparable P_1' group

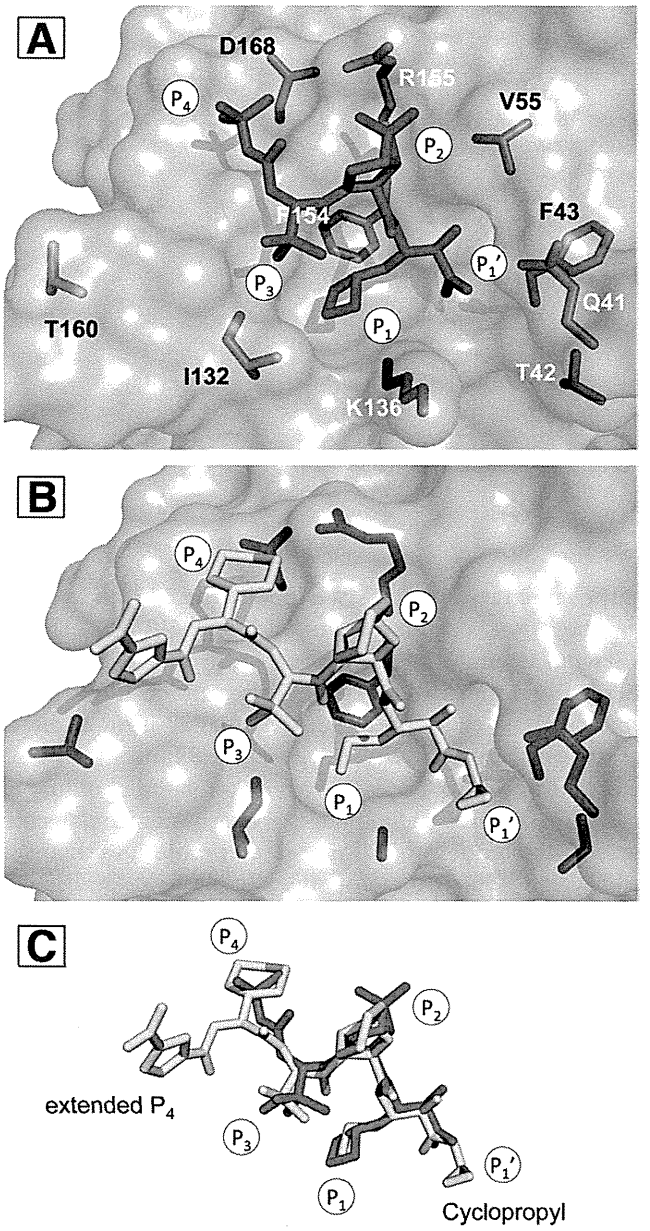

Figure 1. Ligand-binding site of NS3/4A with ketoamides and BSVs. (*A*) Surface representation from PDB structure 2OC8 with boceprevir shown in *magenta*. Side chains at amino acid residues with BSVs are shown in stick format (*light blue*). (*B*) Similar representation of TLL within the PDB structure 2P59 with side chains at amino acid residues with BSVs (*dark blue*). (*C*) Superposition of boceprevir and TLL.

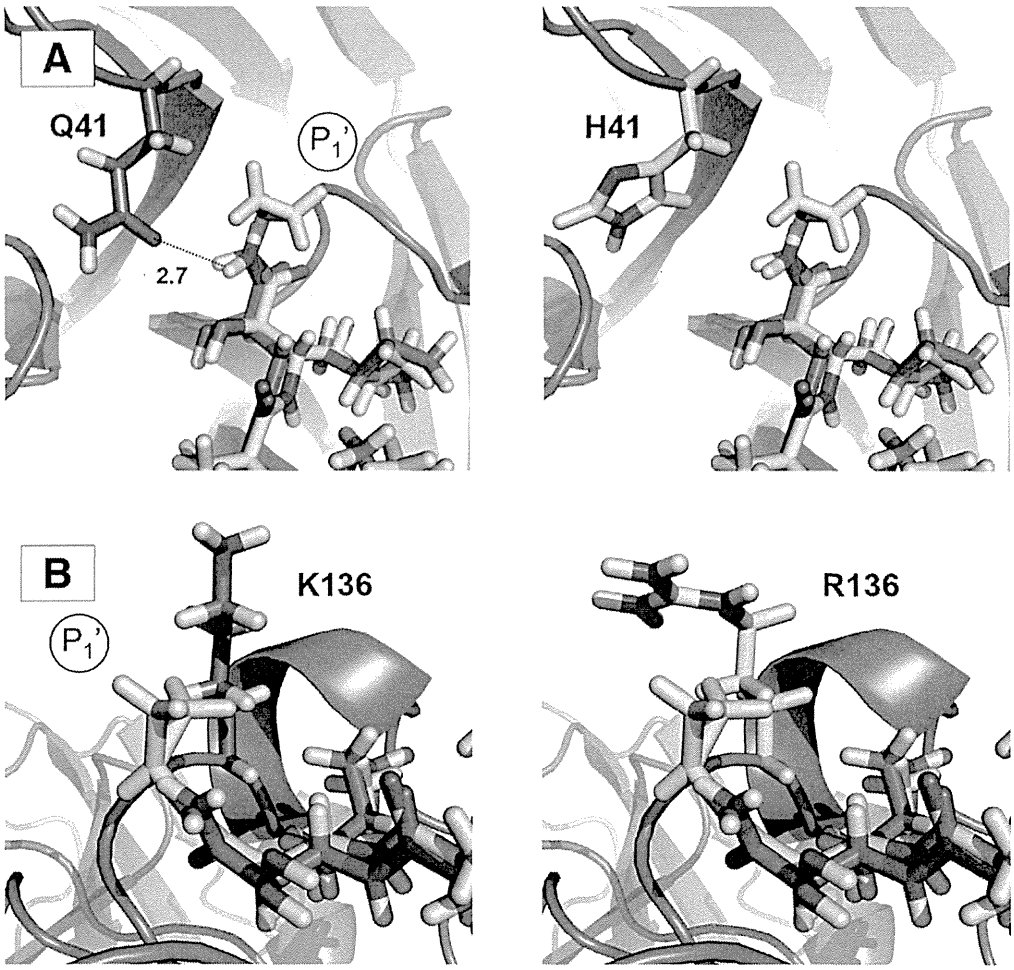

Figure 2. Rotamer analysis of Q41H and K136R. Detail of PDB structure 2OC8 showing boceprevir (*magenta*) and the superposed TLL (*yellow*). Panels on the *left* show the side-chain conformation of the consensus residue, and those on the *right* show the predicted BSV conformation. (*A*) *Left:* The Q41 side-chain OH-group with predicted H-bond interaction (*dotted line*) with ketoamide backbone Cα (*right*), this H-bond interaction is absent in H41. (*B*) Predicted R136 side-chain conformation and the TLL P_1' cyclopropyl showing closer van der Waals contacts in (*right*) R136 than in (*left*) the consensus K136.

(Supplementary Figure 1). We predict the R136 side-chain conformation is similar to the wild-type K136, but that it will wrap around the TLL cyclopropyl group, providing an increasing number of van der Waals contacts (Figure 2*B*). This suggests that the R136 variant may have stronger effects on telaprevir than on boceprevir binding. We expect hydrophilicity to play a role in ketoamide binding at S_1', and the R136 side chain possesses more polar contacts and potentially binds more water molecules than the wild-type K136. Thus, the release of water molecules bound to the R136 side chain could increase systemic entropy and potentially add to the free binding energy and affinity for telaprevir, although decreased enthalpy may compensate for the effects on entropy. Because the R136 side chain does not have a tight H-bond or salt bridge interaction at its end, electrostatic attraction between the nonpolar P_1' cyclopropyl group of telaprevir and the polar R136 side chain is unlikely. Overall, however, the impact of K136R on binding of telaprevir is not readily predicted by rotamer analysis alone.

Expected impact of I132V and F154Y on ketoamide P_1 and P_3 interactions. I132 is located adjacent to S_1 and S_3, and its substitution with valine in V132 represents a conservative change between hydrophobic residues. The consensus I132 side-chain conformation forms a hydrophobic $S_{1/3}$ interface with the ketoamide P_1 and P_3 groups. The I132 side-chain C_δ carbon points toward the ketoamide P_3 group (Figure 3*A*). The variant V132 shows a similar side-chain conformation but without a C_δ carbon. This suggests a loss of van der Waals contacts for V132, resulting in a minor reduction in binding affinity for boceprevir and telaprevir. F154Y is also a relatively conservative change, in this case from nonpolar toward polar, among aromatic residues. This residue is close to the ketoamide P_1 and P_3 groups at the bottom of the S_1 pocket. The wild-type F154 and the predicted variant Y154 side chains are oriented toward the ketoamide P_1 group, potentially influencing boceprevir and telaprevir binding (Figure 3*B*). The Y154 side chain has an OH group that is not present in the wild-type F154. Ketoamides do not offer an opportunity for H-bond interactions at P_1, but this OH group may provide for alternative binding of a water molecule. The polar, hydrophilic nature of the Y154 side chain reduces the hydrophobic properties of the S_1 pocket, and this variant is expected to cause a significant reduction in binding affinity for boceprevir and telaprevir.

Expected impact of R155K, D168E, and D168G on ketoamide P_2 and P_4 interactions. R155K is a conservative change between positively charged residues within the S_2 pocket. The R155 side chain is predicted to participate in a pattern of noncovalent interactions involving its neighboring residues, R123 and D168, at S_4 (the O-H

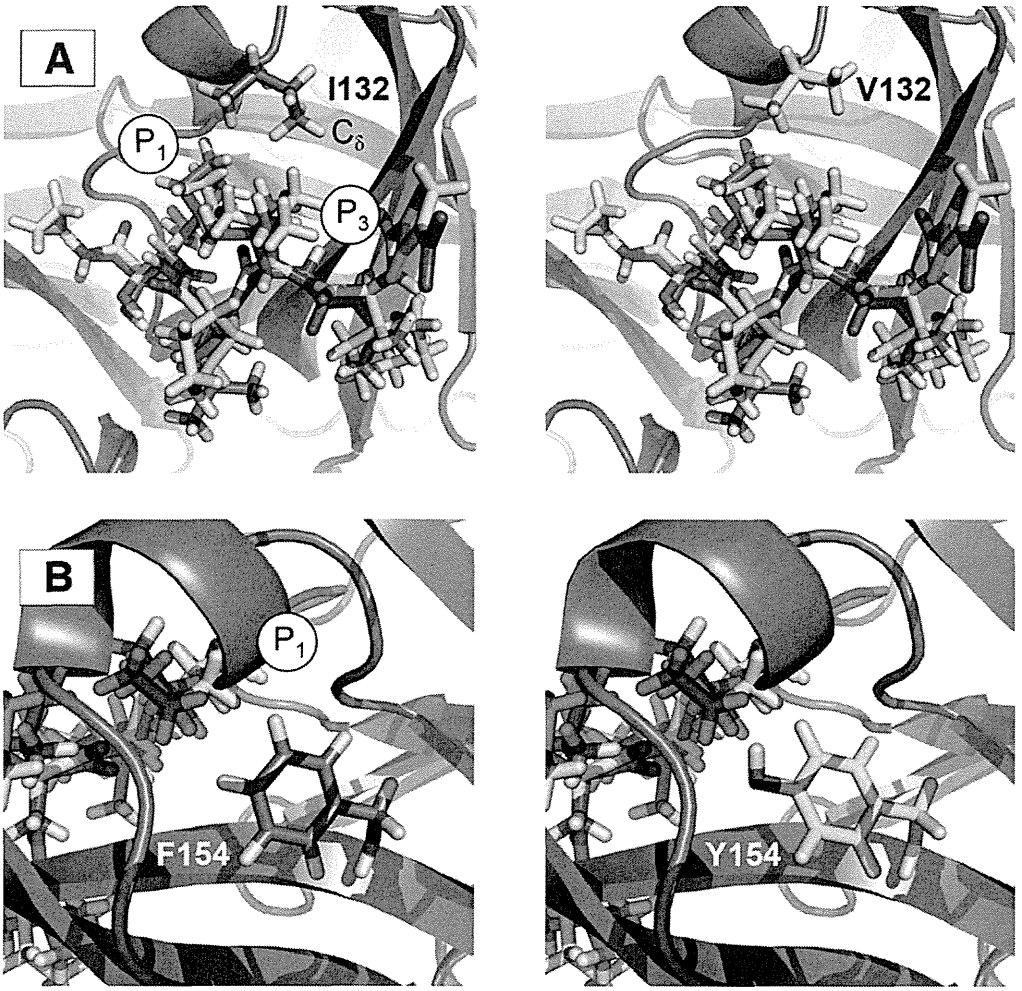

Figure 3. Rotamer analysis of I132V and F154Y. (*A*) *Left*: The I132 side chain provides a hydrophobic $S_{1/3}$ interface for the ketoamide P_1 and P_3 moieties. The I132 C_δ carbon is oriented toward the ketoamide P_3, while (*right*) V132 lacks a C_δ carbon. (*B*) *Left*: F154 neighbors S_1 underneath the ketoamide, while (*right*) Y154 is predicted to assume a similar side-chain conformation but with an additional OH-group.

distance for D168-R155 is 2.6 Å; for R123-D168, it is 2.5 Å) (Figure 4). The combination of H-bond and electrostatic interactions is predicted to result in a particularly strong noncovalent salt bridge interaction. Polar interactions between the D168, R123, and R155 side chains contribute to the strength of this noncovalent interaction network. The D168 side chain is predicted to be tightly fixed, allowing no other H-bond interaction and contributing to a nonpolar $S_{2/4}$ interaction interface for the P_2 and P_4 groups in boceprevir and telaprevir. The variant K155 disrupts this nonpolar $S_{2/4}$ interface by leaving the negatively charged D168 unbound, and is expected to reduce binding affinity for boceprevir and telaprevir. A stronger effect is expected for telaprevir than for boceprevir, because the telaprevir P_2 cyclopental-proline is larger than the respective boceprevir isopropyl-proline (Supple-

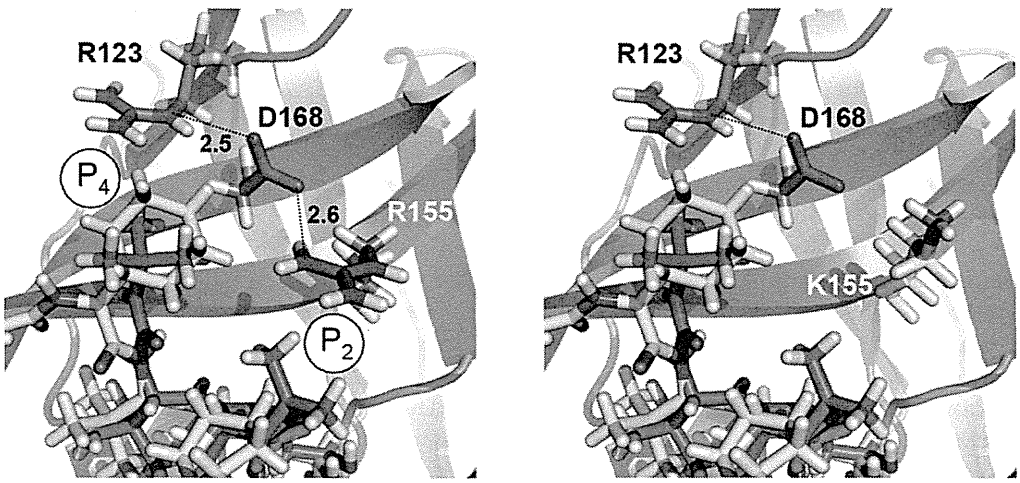

Figure 4. Rotamer analysis of R155K. *Left*: The H-bond pattern (*dotted lines*) in the R155 structure with D168 serving as a nonpolar S_4 contact interface for the ketoamide P_4. *Right*: K155 disables this H-bond pattern, leaving D168 unbound with a polar OH-group at S_4. The K155 side-chain conformation is also predicted to be shifted slightly away from the ketoamide P_2.

mentary Figure 1). Compared with R155, the K155 side chain is also predicted to be shifted slightly away from the ketoamide P_2 group. This shift is likely to cause a loss in van der Waals contacts with the ketoamide P_2 group, and might reduce binding affinity for telaprevir. The effects on polarity and loss of van der Waals contacts suggest that there will be a significant decrease in binding affinity for both ketoamides, but a larger impact on telaprevir.

Two variants were observed at the D168 position that contributes to the S_4 pocket in the protease. D168G is a nonconservative change from aliphatic and polar to a smaller, nonpolar side chain. The wild-type D168 side-chain conformation is oriented toward the ketoamide P_4 group, which is smaller in boceprevir than telaprevir. The extended P_4 group in telaprevir (Figure 1) points away from D168. Thus, the D168 variant is expected to have only minor effects on ketoamide binding. G168 is expected to have effects on the nonpolar $S_{2/4}$ interface similar to K155, because it offers no polar side-chain interaction partner for R155. It is predicted to change the polarity of the $S_{2/4}$ interface and expected to cause a minor decrease in binding affinity for both ketoamides. D168E is a conservative change as both side chains are negatively charged and aliphatic. The side-chain conformation is predicted to be similar to the wild-type D168 and to preserve $S_{2/4}$ interface polarity. D168E is not expected to impact ketoamide binding.

Additional BSVs without expected impact on ketoamide binding. T42A is located at the periphery of the S_1' pocket, and is a nonconservative change from aliphatic, polar, and negative toward aliphatic and hydrophobic. A side-chain OH group is lost in the A42 variant but is preserved in the S42 variant at this position, allowing for a potential H-bond interaction. The wild-type T42 and variant A42 and S42 side-chain conformations are predicted to be similar. No ketoamide H-bond donor or acceptor group is found in close proximity to T42 or S42. Because of its relative distance from the ketoamide, the polarity change in T42A is predicted not to have a significant effect on ketoamide binding. Thus, the T42A/S variants are expected to have no impact on ketoamide binding. F43S is a nonconservative change from aromatic and nonpolar toward aliphatic and polar, and is found at the bottom of S_1'. No change is predicted in the side-chain conformation. There is an additional OH group in the variant, but because there is no ketoamide H-bond donor or acceptor group in close proximity, this by itself is unlikely to have any impact on ketoamide binding. Nevertheless, F43S can cause ketoamide resistance because the F43 aromatic ring directly participates in the formation of the S_1' pocket, which impacts binding of the ketoamide P_1' group.[25] Substitutions at F43 have been shown previously to cause resistance to ketoamide compounds.[25] T160A is a nonconservative change from polar toward nonpolar and hydrophobic, located at a distance from S_4 near the boundary of an extended S_5 pocket. T160 interacts directly with the extended P_4 group in TLL in the PDB structure 2P59, but has no noncovalent interactions with boceprevir in PDB structure 2OC8. The variant A160 side chain is not expected to influence ketoamide binding.

Replication Capacity and Infectious Virus Yield From RNAs Containing BSVs

Those BSVs for which the rotamer analysis suggested a possible impact on ketoamide binding (ie, Q41H, I132V, F154Y, R155K, and D168G) were selected for phenotypic characterization. We similarly tested K136R, for which the rotamer analysis provided no clear predictions. The amino acid substitutions were created within the background of the genotype 1a H77S.3 genome, and their impact on replication of the viral RNA and production of infectious virus determined in RNA-transfected cells.

RNA replication capacity. The replication capacity of H77S.3/GLuc2A RNA mutants with BSV substitutions in NS3 was assessed by measuring GLuc activities in supernatant media collected at 24-h intervals after transfection of synthetic RNA, as described previously.[14] Results were normalized to the activity present at 6 h after transfection, as this represents GLuc expressed directly by the transfected input RNA. The RNA replication capacity of the Q41H variant was similar to the parental H77S.3/

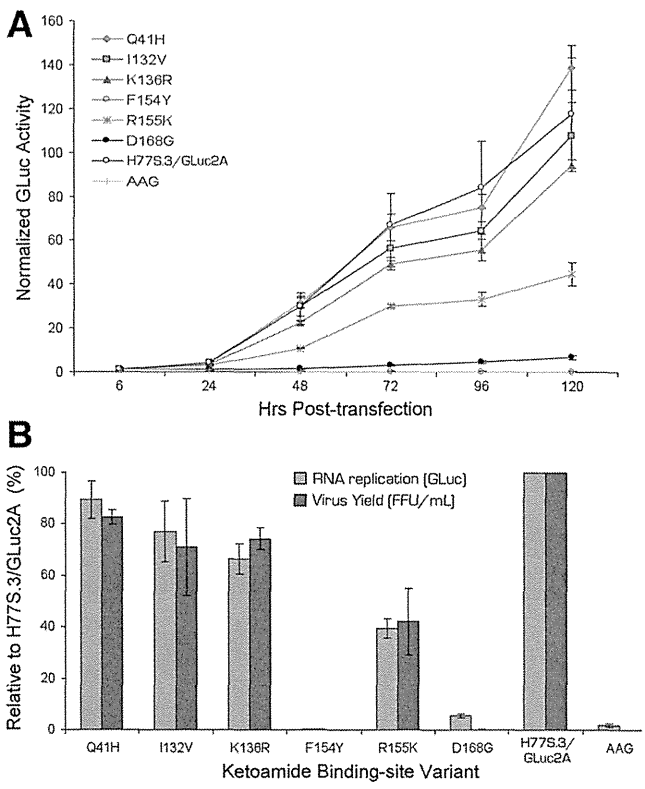

Figure 5. Replication capacity and infectious virus yield of H77S.3 RNAs with BSV substitutions in NS3. (*A*) RNA replication capacity reflected of H77S.3/GLuc2A BSV into Huh7.5 cells. Results are normalized to the 6-h GLuc activity, and represent the mean of triplicate samples. (*B*) Comparison of RNA replication capacity (*lightly shaded bars*) and infectious virus yields (*dark shaded bars*). Both are normalized to those obtained with the relevant parental RNA (100%). Data represent the mean ± SD from at least 3 independent experiments.

Table 2. Predicted and Measured Impact of BSVs on Antiviral Activity of Ketoamides[a]

	IRECS		EC_{50} (nM)		Fold-change in EC_{50}	
Genotype 1a HCV	Boceprevir	TLL	Boceprevir	Telaprevir	Boceprevir	Telaprevir
H77S.3/GLuc2A	–	–	870 (±48)	120 (±10)	1.0	1.0
Q41H	*MiN*[b]	*MiN*	1040 (±60)	410 (±10)	1.2	3.5
T42A	NoI	NoI	–	–	–	–
T42S	NoI	NoI	–	–	–	–
F43S	NoI	NoI	–	–	–	–
I132V	*MiN*	*MiN*	980 (±60)	280 (±40)	1.1	2.4
K136R	NoI	*NP*	440 (±19)	100 (±10)	0.5	0.9
F154Y	*SN*	*SN*	ND	ND	ND	ND
R155K	*MeN*	*SN*	1830 (±240)	1010 (±240)	2.1	8.8
T160A	NoI	NoI	–	–	–	–
D168G	*MiN*	*MeN*	490 (±50)	260 (±30)	0.6	2.2
D168E	NoI	NoI	–	–	–	–

ND, not determined.

[a]The table compares the in silico predictions of the impact of BSVs on ketoamide binding from the Iterative REduction of Conformational Space (IRECS)[20] analysis and corresponding EC_{50} values determined from H77S.3/GLuc2A-transfected cell cultures. Results shown represent the mean ± SD and fold-changes compared with wild-type.

[b]Predicted impact: NoI, no impact; MiN, minor negative impact, change only in a single ketoamide-BSV interaction (H-bond, van der Waals) or in polarity; MeN, moderate negative impact, combined changes in ketoamide-BSV interaction and polarity; SN, strong negative impact, same as for MeN but at particularly close ketoamide-BSV interaction sites; NP, not predictable.

GLuc2A RNA, while I132V and K136R were minimally impaired (Figure 5*A*). In contrast, as shown previously,[14] the replication of R155K was moderately impaired, and D168G was severely handicapped for RNA replication. The maximum RNA replication capacity observed was with Q41H (89% of parental RNA) and the lowest was with D168G (5.5%). The F154Y substitution had a lethal effect on RNA replication in the H77S.3 background, suggesting that viruses containing this sequence variant (and possibly also G168) possess one or more compensating changes at other amino acid positions (see Discussion). None of the BSVs demonstrated enhanced RNA replication capacity compared with the parental H77S.3/GLuc2A RNA (Figure 5*B*).

Infectious virus yield. We also assessed the impact of these BSVs when placed within the background of H77S.3 RNA, which lacks the GLuc2A-coding sequence and produces infectious virus as described previously.[14] Cell culture supernatant fluids were collected 72 h after transfection of the RNA, and subsequently inoculated onto naïve cells, with foci of infected cells detected by immunofluorescence 72 h later. Each of the BSVs tested produced infectious virus yields in the range of that expected from their RNA replication capacity, although the low replication capacity of the D168G variant precluded a careful analysis on production of infectious virus (Figure 5). Thus, none of these amino acid substitutions were documented to directly impair infectious virus assembly or release, as described previously for some resistance-associated NS3 variants.[14] Reductions in the fitness of these particular BSVs are confined primarily to defects in viral RNA replication.

Ketoamide resistance of BSVs. We measured the antiviral activities (50% effective concentration [EC_{50}]) of boceprevir and telaprevir against each of the H77S.3/GLuc2A mutants by determining the concentration of each compound required to cause a 50% reduction in RNA replication (GLuc expression by RNA-transfected cells). Resistance testing could not be performed for the F154Y variant because it was not competent for replication.

Boceprevir demonstrated antiviral activity against each of the BSVs (Table 2). The EC_{50} value against the parental H77S.3/GLuc2A was 870 ± 48 nM. The maximum fold-change in the EC_{50} for any of the BSVs was 2.1 for R155K.[14] Only R155K showed significant, albeit low-level, resistance against boceprevir. Telaprevir showed greater molar activity than boceprevir, with an EC_{50} against the H77S.3/GLuc2A of 120 ± 10 nM. As with boceprevir, telaprevir was active against each of the BSVs, but low- to medium-level resistance was evident with Q41H, I132V, R155K, and D168G (Table 2). The maximum fold-change in the EC_{50} was 8.8 for R155K. As expected from the in silico analysis, the range of fold-changes in EC_{50} was broader for telaprevir than boceprevir. In general, these changes were in good agreement with the impact of these BSVs on ketoamide binding predicted from the rotamer analysis, except for K136R, which was difficult to predict and showed greater antiviral activity than anticipated against both ketoamide compounds (Table 2).

Discussion

Mathematical arguments suggest that every possible drug-resistant viral variant is likely to pre-exist at a low frequency in the replicating viral quasi-species population of the typical HCV-infected patient.[10] Whether this is actually the case, and at what frequency such variants

actually exist, may never be formally demonstrated due to technical difficulties. In this study, we analyzed the natural variation present among ketoamide-neighboring residues in 219 genotype 1a HCV sequences collected from geographically diverse sites and deposited in a public database. We cannot exclude the possibility that some of the BSVs we identified in this set of sequences might represent variants that were present at low frequency in their source patient, or even unrecognized sequencing errors. However, it is likely that they represent true variants present within the dominant quasi-species of the patients from whom these sequences were derived, because multiple BSVs were identified at some residues (T42, V55, and D168) (Supplementary Figure 2), while others (H41, A42, A55, I44, and K155) were present in more than one sequence. We identified BSVs at one or more ketoamide-neighboring residues in 17 of 219 (7.8%) genotype 1a sequences. Importantly, 8 of these variants (Q41H, T42A, T42S, V55I, I132V, K136R, F154Y, and T160A) have not been identified, to our knowledge, in previous in vivo or in vitro studies of ketoamide resistance.

Although they are both linear ketoamide compounds, boceprevir and telaprevir have distinct structural features (Supplementary Figure 1). Telaprevir possesses an extended P_4 capping group and a P_1' cyclopropyl group. The P_2 group is different from the isopropyl-proline in boceprevir, which is smaller than the telaprevir P_2 cyclopentalproline.[23] These structural differences likely contribute to the lower EC_{50} of telaprevir against genotype 1a HCV in cell culture (Table 2), but could also pose a higher risk for telaprevir resistance among BSVs. Rotamer analysis predicted that 2 BSVs (R155K and D168G) would exert a greater negative effect on the binding of telaprevir than boceprevir. The impact of the K136R substitution proved difficult to predict on the basis of rotamer analysis alone, however, and subsequent tests in cell culture demonstrated that it imposes no resistance against either ketoamide (Table 2).

On the other hand, the R155K and D168G substitutions led to a 2- to 4-fold greater increase in the EC_{50} of teleprevir compared with boceprevir, and an almost 9-fold increase in the teleprevir EC_{50}. This was consistent with predictions from the rotamer analysis, which also agreed with previous crystallographic studies.[26] Whether such changes in the EC_{50} result in clinical resistance would be dependent on the potency of a drug and the drug exposure achieved in a typical patient. A 2-fold change might not be clinically relevant, but a 9-fold increase such as that found with R155K is likely to be significant. Importantly, R155K has been associated previously with resistance to both ketoamide and macrocyclic compounds.[23,26]

Three BSVs (Q41H, I132V, and F154Y) were predicted to interact with ketoamide structural features common to both telaprevir and boceprevir, and thus to influence the binding of these compounds equally. Although Q41H was expected to cause only a minor decrease in affinity for both ketoamides, in vitro assays revealed a 3.5-fold increase in the EC_{50} for teleprevir vs 1.2 for boceprevir. Its greater impact on telaprevir potency is likely related to its P_1' cyclopropyl group and induced structural changes in the corresponding S_1' pocket. Such changes were not detectable using rotamer analysis, but probably influenced the binding of telaprevir. A similar difference in the magnitude of the change in EC_{50} was observed for the I132V variant (1.1-fold change for boceprevir vs 2.4-fold for teleprevir). This could result from a loss of van der Waals contacts with the ketoamide P_3 group, which differs slightly in its orientation in the co-crystallized boceprevir and TLL structures (see Figure 1). The F154Y substitution was lethal for RNA replication when placed in the background of the H77S.3 virus, and thus we could not measure antiviral activity against it.

Viral fitness coupled with the degree of resistance conferred by a BSV are likely to be the major determinants driving selection of a variant from within the viral quasi-species during therapy. RNA replication capacity is one measure of the fitness of the virus, and this is dependent on proper processing of the polyprotein by NS3/4A. Ketoamides mimic the natural substrate of the protease at the site of NS3-NS4A scission, and it is likely that the negative influence of BSVs on RNA replication (Figure 5*A*) reflects altered recognition of the polyprotein substrate related to structural changes similar to those leading to drug resistance. Despite this, there is no strong correlation between the degree of PI resistance and the impact on RNA replication.[14] This is reflected in the marked deficit in replication demonstrated by the D168G substitution (Figure 1*A*), which confers only a minimal increase in the teleprevir EC_{50} (Table 2). There is no obvious structural or molecular explanation for this difference, and it is not possible to exclude the possibility that G168 might provide for more robust RNA replication when placed in the context of a different virus sequence.

In contrast, F154Y was lethal for replication in the context of the H77S.3 virus. This substitution occurs at a central position within the ligand-binding site at the bottom of the S_1 pocket. A recent crystallographic study found the F154 aromatic ring to directly contact the substrate P_1 side chain.[27] Thus, the complete loss of RNA replication observed with F154Y could be due to either intrusion of the Y154 side chain into the space normally occupied by the polyprotein substrate, or a polarity shift within S_1 due to the Y154 OH group.

The presence of Y154 in the database suggests that it is capable of functioning in an alternative sequence context. This highlights a limitation of the technical approach we have taken here to study the phenotypic effect of BSVs, as second-site substitutions in the same strain might compensate for defects fitness. In fact, the sequence of the F154Y BSV (EU677253) contains 2 additional substitutions in NS3 that differ from the genotype 1a consensus: R11G and H110R (Supplemen-

tary Figure 2). H110R is in close structural proximity to F154Y and the natural substrate of the protease (Supplementary Figure 3). Although it might be preferable when investigating BSVs to engineer swaps of the complete NS3 sequence into the background of a replication-competent clone, it is not clear how often this approach would fail due to sequence incompatibilities between the donor and recipient viruses. NS3 appears to interact with several other viral proteins.[28]

Our findings provide a molecular basis for ketoamide resistance among BSVs that exist naturally as dominant quasi-species in some patients before treatment with DAAs (Supplementary Table 3). Such natural variants might be of limited clinical significance at present because they are likely to be suppressed by Peg-IFN/RBV in current SOC regimens, but they can be expected to be of substantial importance to the outcome of future interferon-sparing, all-DAA combination therapies. These variants might also affect future generations of inhibitors depending on their chemical structures. Knowledge on the natural variability in structures targeted by antivirals, as presented in this study, can help guide the development of future generation PIs.

Supplementary Material

Note: To access the supplementary material accompanying this article, visit the online version of *Gastroenterology* at www.gastrojournal.org, and at doi: 10.1053/j.gastro.2011.11.035.

References

1. Fried MW, Shiffman ML, Reddy KR, et al. Peginterferon alfa-2a plus ribavirin for chronic hepatitis C virus infection. N Engl J Med 2002;347:975–982.
2. Manns MP, McHutchison JG, Gordon SC, et al. Peginterferon alfa-2b plus ribavirin compared with interferon alfa-2b plus ribavirin for initial treatment of chronic hepatitis C: a randomised trial. Lancet 2001;358:958–965.
3. Shiffman ML, Suter F, Bacon BR, et al. Peginterferon alfa-2a and ribavirin for 16 or 24 weeks in HCV genotype 2 or 3. N Engl J Med 2007;357:124–134.
4. Malcolm BA, Liu R, Lahser F, et al. SCH 503034, a mechanism-based inhibitor of hepatitis C virus NS3 protease, suppresses polyprotein maturation and enhances the antiviral activity of alpha interferon in replicon cells. Antimicrob Agents Chemother 2006; 50:1013–1020.
5. Prongay AJ, Guo Z, Yao N, et al. Discovery of the HCV NS3/4A protease inhibitor (1R,5S)-N-[3-amino-1-(cyclobutylmethyl)-2,3-dioxopropyl]-3-[2(S)-[[[(1,1-dimethylethyl)amino]carbonyl]amino]-3,3-dimethyl-1-oxobutyl]-6,6-dimethyl-3-azabicyclo[3.1.0]hexan-2(S)-carboxamide (Sch 503034) II. Key steps in structure-based optimization. J Med Chem 2007;50:2310–2318.
6. Perni RB, Almquist SJ, Byrn RA, et al. Preclinical profile of VX-950, a potent, selective, and orally bioavailable inhibitor of hepatitis C virus NS3-4A serine protease. Antimicrob Agents Chemother 2006;50:899–909.
7. Hezode C, Forestier N, Dusheiko G, et al. Telaprevir and peginterferon with or without ribavirin for chronic HCV infection. N Engl J Med 2009;360:1839–1850.
8. Kwo PY, Lawitz EJ, McCone J, et al. Efficacy of boceprevir, an NS3 protease inhibitor, in combination with peginterferon alfa-2b and ribavirin in treatment-naive patients with genotype 1 hepatitis C infection (SPRINT-1): an open-label, randomised, multicentre phase 2 trial. Lancet 2010;376:705–716.
9. McHutchison JG, Everson GT, Gordon SC, et al. Telaprevir with peginterferon and ribavirin for chronic HCV genotype 1 infection. N Engl J Med 2009;360:1827–1838.
10. Rong L, Dahari H, Ribeiro RM, et al. Rapid emergence of protease inhibitor resistance in hepatitis C virus. Sci Transl Med 2010;2: 30ra32.
11. Neumann AU, Lam NP, Dahari H, et al. Hepatitis C viral dynamics in vivo and the antiviral efficacy of interferon-alpha therapy. Science 1998;282:103–107.
12. Raney KD, Sharma SD, Moustafa IM, et al. Hepatitis C virus non-structural protein 3 (HCV NS3): a multifunctional antiviral target. J Biol Chem 2010;285:22725–22731.
13. Kolykhalov AA, Mihalik K, Feinstone SM, et al. Hepatitis C virus-encoded enzymatic activities and conserved RNA elements in the 3′ nontranslated region are essential for virus replication in vivo. J Virol 2000;74:2046–2051.
14. Shimakami T, Welsch C, Yamane D, et al. Protease inhibitor-resistant hepatitis C virus mutants with reduced fitness from impaired production of infectious virus. Gastroenterology 2011; 140:667–675.
15. Ma Y, Yates J, Liang Y, et al. NS3 helicase domains involved in infectious intracellular hepatitis C virus particle assembly. J Virol 2008;82:7624–7639.
16. Yi M, Tong X, Skelton A, et al. Mutations conferring resistance to SCH6, a novel hepatitis C virus NS3/4A protease inhibitor: reduced RNA replication fitness and partial rescue by second-site mutations. J Biol Chem 2006;281:8205–8215.
17. Kouranov A, Xie L, de la Cruz J, et al. The RCSB PDB information portal for structural genomics. Nucleic Acids Res 2006;34:D302–D305.
18. Schechter I, Berger A. On the size of the active site in proteases. I. Papain. Biochem Biophys Res Commun 1967;27:157–162.
19. Combet C, Garnier N, Charavay C, et al. euHCVdb: the European hepatitis C virus database. Nucleic Acids Res 2007;35:D363–D366.
20. Hartmann C, Antes I, Lengauer T. IRECS: a new algorithm for the selection of most probable ensembles of side-chain conformations in protein models. Protein Sci 2007;16:1294–1307.
21. Prongay AJ, Guo Z, Yao N, et al. Discovery of the HCV NS3/4A protease inhibitor (1R,5S)-N-[3-amino-1-(cyclobutylmethyl)-2,3-dioxopropyl]-3-[2(S)-[[[(1,1-dimethylethyl)amino]carbonyl]amino]-3,3-dimethyl-1-oxobutyl]-6,6-dimethyl-3-azabicyclo[3.1.0]hexan-2(S)-carboxamide (Sch 503034) II. Key steps in structure-based optimization. J Med Chem 2007;50:2310–2318.
22. Perni RB, Chandorkar G, Cottrell KM, et al. Inhibitors of hepatitis C virus NS3.4A protease. Effect of P4 capping groups on inhibitory potency and pharmacokinetics. Bioorg Med Chem Lett 2007;17: 3406–3411.
23. Tong X, Bogen S, Chase R, et al. Characterization of resistance mutations against HCV ketoamide protease inhibitors. Antiviral Res 2008;77:177–185.
24. Susser S, Welsch C, Wang Y, et al. Characterization of resistance to the protease inhibitor boceprevir in hepatitis C virus-infected patients. Hepatology 2009;50:1709–1718.
25. Welsch C, Domingues FS, Susser S, et al. Molecular basis of telaprevir resistance due to V36 and T54 mutations in the NS3-4A protease of the hepatitis C virus. Genome Biol 2008;9:R16.
26. Zhou Y, Muh U, Hanzelka BL, et al. Phenotypic and structural analyses of hepatitis C virus NS3 protease Arg155 variants: sensitivity to telaprevir (VX-950) and interferon alpha. J Biol Chem 2007;282:22619–22628.
27. Romano KP, Ali A, Royer WE, et al. Drug resistance against HCV NS3/4A inhibitors is defined by the balance of substrate recognition versus inhibitor binding. Proc Natl Acad Sci U S A 2010;107: 20986–20991.
28. Ma Y, Anantpadma M, Timpe JM, et al. Hepatitis C virus NS2 protein serves as a scaffold for virus assembly by interacting with both structural and nonstructural proteins. J Virol 2011;85:86–97.

Received July 5, 2011. Accepted November 29, 2011.

Reprint requests

Address requests for reprints to: Christoph Welsch, MD, Department of Medicine, Inflammatory Disease Institute and the Lineberger Comprehensive Cancer Center, CB#7030, The University of North Carolina at Chapel Hill, Chapel Hill, North Carolina 27599-7292. e-mail: christophwelsch@gmx.net; fax: (919) 843-7240.

Acknowledgments

The authors thank Ann D. Kwong and Govinda Rao for their critical reading of this article.

Conflicts of interest

These authors disclose the following: Stefan Zeuzem has served as a consultant for Abbott, Achillion, Anadys, BMS, Boehringer, Gilead, iTherX, Janssen, Merck, Novartis, Pfizer, Pharmasset, Roche, Santaris, Tibotec, and Vertex. Stanley M. Lemon has served as a consultant for Abbott, Hoffmann-LaRoche, Juvaris Biotherapeutics, Merck, Novartis, and Pfizer; research in his laboratory is supported by Merck and Tibotec. The remaining authors disclose no conflicts.

Funding

This study was supported by a Deutsche Forschungsgemeinschaft grant to CW, TL, and SZ (Clinical Research Unit, KFO129, TP3 and TP6, LE 491/16-2 and LE 491/17-2) and a Deutsche Forschungsgemeinschaft Research Fellowship (WE 4388/3-1) to CW. SML was supported by the National Institutes of Health (NO1-AI25488, RO1-AI095690).